103: 3412-3419.

16) Dooriss KL, Denning G, Gangadharan B, et al. Comparison of Factor VIII Transgenes Bioengineered for Improved Expression in Gene Therapy of Hemophilia A. Hum Gene Ther. 2009; **20**: 465-478.
17) Ward NJ, Buckley SM, Waddington SN, et al. Codon optimization of human factor VIII cDNAs leads to high-level expression. Blood. 2011; **117**: 798-807.
18) Margaritis P, Roy E, Aljamali MN, et al. Successful treatment of canine hemophilia by continuous expression of canine FVIIa. Blood. 2009; **113**: 3682-3689.
19) Kren BT, Unger GM, Sjeklocha L, et al. Nanocapsule-delivered Sleeping Beauty mediates therapeutic Factor VIII expression in liver sinusoidal endothelial cells of hemophilia A mice. J Clin Invest. 2009; **119**: 2086-2099.
20) Wang Z, Ma HI, Li J, Sun L, Zhang J, Xiao X. Rapid and highly efficient transduction by double-stranded adeno-associated virus vectors *in vitro* and *in vivo*. Gene Ther. 2003; **10**: 2105-2111.
21) Ishiwata A, Mimuro J, Mizukami H, et al. Mutant macaque factor IX T262A: a tool for hemophilia B gene therapy studies in macaques. Thromb Res. 2010; **125**: 533-537.
22) Nathwani AC, Gray JT, McIntosh J, et al. Safe and efficient transduction of the liver after peripheral vein infusion of self-complementary AAV vector results in stable therapeutic expression of human FIX in nonhuman primates. Blood. 2007; **109**: 1414-1421.
23) Calcedo R, Vandenberghe LH, Gao G, Lin J, Wilson JM. Worldwide epidemiology of neutralizing antibodies to adeno-associated viruses. J Infect Dis. 2009; **199**: 381-390.
24) Nathwani AC, Davidoff AM, Hanawa H, et al. Sustained high-level expression of human factor IX (hFIX) after liver-targeted delivery of recombinant adeno-associated virus encoding the hFIX gene in rhesus macaques. Blood. 2002; **100**: 1662-1669.
25) Nathwani AC, Gray JT, Ng CY, et al. Self-complementary adeno-associated virus vectors containing a novel liver-specific human factor IX expression cassette enable highly efficient transduction of murine and nonhuman primate liver. Blood. 2006; **107**: 2653-2661.
26) Nathwani A, Tuddenham E, Rosales C, et al. Early Clinical Trial Results Following Administration of a Low Dose of a Novel Self Complementary Adeno-Associated Viral Vector Encoding Human Factor IX In Two Subjects with Severe Hemophilia B [abstract]. Blood. 2010; **116**: 114. Abstract 248.

Thrombosis Research 128 (2011) 283–292

Contents lists available at ScienceDirect

Thrombosis Research

journal homepage: www.elsevier.com/locate/thromres

Regular Article

Local regulation of neutrophil elastase activity by endogenous α1-antitrypsin in lipopolysaccharide-primed hematological cells

Momoko Dokai, Seiji Madoiwa *, Atsushi Yasumoto, Yuji Kashiwakura, Akira Ishiwata, Asuka Sakata, Nobuko Makino, Tsukasa Ohmori, Jun Mimuro, Yoichi Sakata *

Research Divisions of Cell and Molecular Medicine, School of Medicine, Jichi Medical University, Shimotsuke, Tochigi, Japan

ARTICLE INFO

Article history:
Received 10 November 2010
Received in revised form 14 April 2011
Accepted 26 April 2011
Available online 31 May 2011

Keywords:
Neutrophil elastase
α1-antitrypsin
LPS
siRNA

ABSTRACT

Neutrophil elastase released from activated neutrophils contributes in combating bacterial infection. While chronic inflammation results in anemia and decreased bone marrow activities, little is known about the effect of neutrophil elastase on hematological cell growth in severe inflammatory states. Here, we demonstrated that α1-antitrypsin, a physiological inhibitor of neutrophil elastase, functions as a regulator for cell growth by neutralizing neutrophil elastase activity in lipopolysaccharide-primed hematological cells. HL-60 cells were resistant to neutrophil elastase, as they also expressed α1-antitrypsin. The growth of HL-60 cells transduced with a LentiLox-short hairpin α1-antitrypsin vector was significantly suppressed by neutrophil elastase or lipopolysaccharide. When $CD34^+$ progenitor cells were differentiated towards a granulocytic lineage, they concomitantly expressed neutrophil elastase and α1-antitrypsin and prevented neutrophil elastase-induced growth inhibition. These results suggest that granulocytes might protect themselves from neutrophil elastase-induced cellular damage by efficiently neutralizing its activity through the simultaneous secretion of endogenous α1-antitrypsin.

Introduction

Neutrophil elastase is implicated in antimicrobial defense by degrading engulfed microorganisms [1–4]. Neutrophil elastase is a potent protease as it cleaves almost all connective tissue components as well as soluble proteins [5–7]. At the site of inflammation, neutrophil elastase released from azurophilic granules of the activated leukocyte is thought to mediate tissue destruction through its proteolytic cleavage of cell surface glycoproteins, extracellular matrix and junctional complexes [5,8]. The activity of neutrophil elastase is counteracted by endogenous inhibitors [9–11]. The serine protease inhibitor, α1-antitrypsin possesses potent anti-neutrophil elastase activities [12]. Abnormalities of α1-antitrypsin have been associated with liver damage arising from pathologic polymerization of the variant α1-antitrypsin, and with the development of pulmonary emphysema or panniculitis due to inflammatory stimuli leading to the unregulated activity of neutrophil elastase [13–16].

Neutrophil elastase is also known to provide feedback to granulopoiesis through direct proteolytic action on granulocyte-colony stimulating factor (G-CSF) [17]. Patients with mutations in the gene encoding neutrophil elastase (ELANE) display severe congenital neutropenia due to abnormal traffic of neutrophil elastase and induction of the unfolded protein response [18–20]. In addition, neutrophil elastase induces apoptosis of hematopoietic progenitor cells, which is prevented by a secretory proteinase inhibitor [17,21]. Chronic infection or inflammation results in anemia and decreased bone marrow activities [22,23], and hematopoietic efficacy declines with hematopoietic cell apoptosis and altered cytokine production [24,25]. However, little is known regarding the effect of neutrophil elastase on hematological cell growth or regulation by α1-antitrypsin in severe inflammatory states such as sepsis.

In this study, we investigated the possibility that the growth of hematological cells may be affected by the enzymatic activity of neutrophil elastase and that is regulated by endogenous alpha1-antitrypsin under the stimulation of lipopolysaccharide.

Materials and methods

Cell lines and cell cultures

The human leukemia cell lines HL-60 and K562 were obtained from the American Type Culture Collection (ATCC, Manassas VA, USA) and MEG-01 was purchased from the European Collection of Cell Cultures (ECACC, Down, UK). They were cultured in RPMI 1640 medium (Gibco BRL, Rockville, MD, USA) supplemented with 10% heat-inactivated FBS (Gibco). Cells were adapted to serum free AIM-V Medium (Gibco) as needed. Human embryonic kidney 293 T cells

* Corresponding authors at: Research Division of Cell and Molecular Medicine, Center for Molecular Medicine, Jichi Medical University, 3311-1 Yakushi-ji, Shimotsuke, Tochigi 329-0498, Japan. Tel.: +81 285 58 7398; fax: +81 285 44 7817.
E-mail address: madochan@jichi.ac.jp (S. Madoiwa).

0049-3848/$ – see front matter © 2011 Elsevier Ltd. All rights reserved.
doi:10.1016/j.thromres.2011.04.024

were also purchased from the ATCC and grown in DMEM/F-12 medium (Gibco) supplemented with 10% heat-inactivated FBS. Human cord blood cells were isolated from healthy volunteers with informed consents according to the Declaration of Helsinki.

In vitro differentiation of human cord blood derived CD34$^+$ cells

Human cord blood-derived CD34$^+$ progenitor cells from four independent donors were isolated with a CD34 MicroBead Kit (Miltenyi Biotech, Auburn, CA, USA), and cultured with StemPro-34 SFM (Invitrogen, San Diego, CA, USA). These cells were differentiated into three lineages of hematological cells using appropriate cytokines: granulocytic (10 ng/mL GM-CSF, 10 ng/mL IL-3, and 50 ng/mL SCF), erythrocytic (3 U/mL EPO, 10 ng/mL IL-3 and 50 ng/mL SCF) and megakaryocytic (50 ng/mL TPO, 10 ng/mL IL-3, and 10 ng/mL IL-6) [26].

Measurement of neutrophil elastase activity

The enzymatic activity of neutrophil elastase was determined by an amidolytic reaction to a specific substrate, methoxysuc-AAPV-p-nitroanilide (Sigma-Aldrich, St. Louis, MO, USA) and measuring its absorbance at 405 nm with a Bechmark Plus Spectrophotometer (Bio-Rad Laboratories, Hercules, CA, USA), as previously described [27].

Detection of human neutrophil elastase mRNA and related factor mRNA

RNA samples were subjected to reverse transcription-polymerase chain reaction (RT-PCR) using the following primer pairs: neutrophil elastase forward (5'-GTAAACTTGCTCAACGACATC-3') and reverse (5'-CTCACGAGAGTGCAGACGTT-3'); α1-antitrypsin forward (5'-CAGATCAACGATTACGTGGAGA-3') and reverse (5'-GCTTCATCATAGGGACCTTCAC-3'); and GAPDH forward (5'-AAGGTGAAGGTCGGAGTC-3') and reverse (5'-GAAGATGGTGATGGGATTTC-3'). The RT-PCR was performed using a GeneAmp RNA PCR Core kit (Applied Biosystems, Foster City, CA, USA) as previously described. In brief, reverse transcription was performed at 42 °C for 30 minutes followed by PCR. The initial denaturation step was at 95 °C for 5 minutes followed by 30 cycles of denaturation at 95 °C for 15 seconds, annealing at 58 °C for 30 seconds, and extension at 72 °C for 7 seconds.

Construction of lentiviral α1-antitrypsin shRNAi vectors

To knock down α1-antitrypsin, shRNAi vectors were constructed. As a control, a scramble sequence was inserted into the vector used. The piGENE hU6 vector (iGENE Therapeutics, Tokyo, Japan) was digested with the restriction enzymes Eco*RI* (Toyobo, Osaka, Japan) and Hind*III* (Fermentas Life Sciences, Ontario, Canada). The fragment incorporating the hU6 promoter and a BfuAI site was extracted with a MinElute Gel Extraction Kit (QIAGEN, Valencia, CA, USA) and inserted into the pBC SK + vector (Stratagene, La Jolla, CA, USA), linearized with *Eco*RI and *Hind*III. After digestion with *Xba*I and *Xho*I (Toyobo), they were cut and inserted into the pLentiLox 3.7 vector (pLL3.7 vector; ATCC) previously treated with *Xba*I and *Xho*I. Short interfering RNAs (siRNAs) targeted towards human α1-antitrypsin were based on sequences within the NCBI database. Sense and antisense oligonucleotides of siRNA were designed by Hokkaido System Science (Sapporo, Japan). The sequences oligonucleotides used in this study were: short hairpin sense (5'-CACCGTTTGGGTATGTTTAGCATACGTGTGCTGTCCGTATGTTAAACATGCCTAAACTTTTT-3') and antisense (5'-GCATAAAAAGTTTAGGCATGTTTAACATACGGACAGCACACGTATGCTAAACATACCCAAAC-3'); scramble sense (5'-CACCGATCATAGATAGCACAGGTACGTGTGCTGTCCGTACTTGTGCTATCTGTGGTCTTTTT-3') and antisense (5'-GCATAAAAAGACCACAGATAGCACAAGTACGGACAGCACACGTACCTGTGCTATCTATGATC-3'). These oligonucleotides were ligated into pLL3.7 at the *Bfu*AI site. The pLL3.7 shRNAi plasmid was co-transfected with three plasmids containing PV, REV and VSV-G into 293 T cells. Viral RNA was purified using a QIAamp Viral RNA Mini kit (QIAGEN), and the number of viral particles was determined with a TaqMan PCR Core reagent kit (Applied Biosystems) and an ABI 7700 System (Applied Biosystems). The primers used for quantitative RT-PCR analysis were: forward (5'-GCTTTCATTTTCTCCTCCTT-3') and reverse (5'-GGCCACAACTCCTCATAA-3') along with a FAM-labeled probe (5'-ATCCTGGTTGCTGTCT-3').

Stimulation of hematological cells with neutrophil elastase or lipopolysaccharide (LPS)

Cultured hematological cells were treated with various concentrations of neutrophil elastase (Elastin Products, Owensville, MO, USA), α1-antitrypsin (Sigma-Aldrich) and sivelestat sodium hydrate (ONO Pharma, Osaka, Japan). For LPS stimulation, 1×10^6 cells were incubated with 10 ng/mL LPS (Sigma-Aldrich) at 37 °C for 45 minutes. After washing, cells were re-suspended in the medium with 100 nM N-formyl-Met-Leu-Phe (fMLP; Sigma-Aldrich) for another 45 minutes at 37 °C, as described previously [28].

Western blot analysis

Cells were lysed with a lysis buffer (10 mM Tris-HCl pH 7.6, 1% NP40, 0.15 M NaCl, 1 mM EDTA, 10 μg/mL aprotinin), and each sample consisted of 1×10^6 cells. After centrifugation, 10 μg of sample was applied to SDS-PAGE then electrically transferred to PVDF membranes. After blocking with 20 mM Tris-HCl, (pH 7.6) and 150 mM NaCl containing 2% bovine serum albumin (BSA) at 25 °C for 1 hour, the membrane was incubated with mouse anti-human α1-antitrypsin antibody (1:3000; Ikagaku, Kyoto, Japan) followed by goat anti-mouse IgG horseradish peroxidase-conjugated antibody (1:10000; Invitrogen) in 20 mM Tris-HCl, (pH 7.6), 150 mM NaCl containing 0.1% Tween20 for detection by an ECL Western Blot Detection system (GE Healthcare, Buckinghamshire, UK).

Enzyme-linked immunosorbent assays (ELISAs)

The levels of neutrophil elastase antigen were measured using a Human Elastase ELISA kit from Hycult biotechnology (Uden, Netherlands). The α1-antitrypsin antigen levels were measured using an AssayMax Human α1-Antitripsin Elisa Kit from Assaypro (St. Charles, MO, USA). Concentrations of transforming growth factor-β1 (TGF-β1) were determined by a Quantikine Human TGF-β1 Immunoassay kit from R&D Systems (Minneapolis, MN, USA). The manufacturer's recommended protocols were followed for each kit.

Immunohistochemistry

Cytospin slides containing 1×10^5 cells were prepared with a Cytospin3 (Shandon, Cheshire, UK). After fixation with ethanol, they were incubated with phosphate-buffered saline (PBS) containing 1% BSA and 1% non-immune goat serum for 10 minutes at 25 °C. After blocking, slides were stained for 2 hours at 4 °C using a rabbit anti-human neutrophil elastase antibody (1:200; Calbiochem, Darmstadt, Germany) or mouse anti-human α1-antitrypsin antibody (1:200; Ikagaku) diluted with PBS containing 1% BSA as primary reagents. After washing with PBS, they were incubated with Alexa Fluor-488 labeled goat anti-rabbit IgG antibody (1:500; Invitrogen) or Alexa Fluor-555 conjugated rabbit anti-mouse IgG antibody (1:500; Invitrogen) for 1 hour at 25 °C. Nuclei were stained with DAPI (Roche, Basel, Switzerland).

Terminal dUTP nick-end labeling (TUNEL) Assay

Cytospin slides with 1×10^5 cells were fixed with ethanol, and the TUNEL assay was performed using the DeadEnd Colorimetric

Apoptosis Detection System (Promega, Madison, WI, USA) according to the manufacturer's protocol. Quantification of TUNEL positive cells was determined by mean percentage of apoptotic cells from the total number of cells counted in five fields per slide.

Statistical analysis

The SPSS statistical software package (SPSS, Chicago, IL, USA) was used for all statistical analyses of data. Variables not normally distributed were analyzed with the two-sided Mann-Whitney *U* test. A difference with $p<0.03$ was considered statistically significant.

Results

Effect of LPS on secretion of neutrophil elastase and proliferation in hematological cells

We stimulated three different hematological cell types, HL-60, K562 and MEG-01 cells with LPS. The antigen levels of neutrophil elastase were increased only in HL-60 cells (Fig. 1 A). However, the enzymatic activity of neutrophil elastase was markedly decreased until four hours after the stimulation (Fig. 1 B). LPS did not affect proliferation of any cell type (Fig. 1 C). Then, we cultured 1×10^5 cells/mL of HL-60, K562 and MEG-01 for 24 hours in the absence or presence of the supernatants derived from HL-60 cells that had been stimulated with 10 ng/mL LPS for one hour. Interestingly, the proliferation of K562 and MEG-01 cells was markedly inhibited in the presence of culture medium derived from LPS-stimulated HL-60 cells, although their supernatants did not suppress proliferation of naïve HL-60 cells (Fig. 1 D). These inhibitory effects on K562 and MEG-01 cells were canceled by a human neutrophil elastase specific inhibitor, sivelestat sodium (Fig. 1 D).

Effect of neutrophil elastase on proliferation of hematological cells

To determine whether neutrophil elastase could inhibit proliferation of hematological cells, HL-60, K562 and MEG-01 cells were cultured in the presence of neutrophil elastase. Proliferation of K562 and MEG-01 was significantly inhibited by treating with 1 nM neutrophil elastase for 72 hours (Fig. 2 A), and their proliferation was suppressed in a dose-dependent manner (Fig. 2 B). In contrast, neutrophil elastase had no effect on the proliferation of HL-60 cells. Both K562 and MEG-01 underwent apoptosis in a dose-dependent manner with neutrophil elastase (Fig. 2 C and D). There was no significant increase in the number of apoptotic cells when HL-60 cells were cultured in the presence of 5 nM neutrophil elastase.

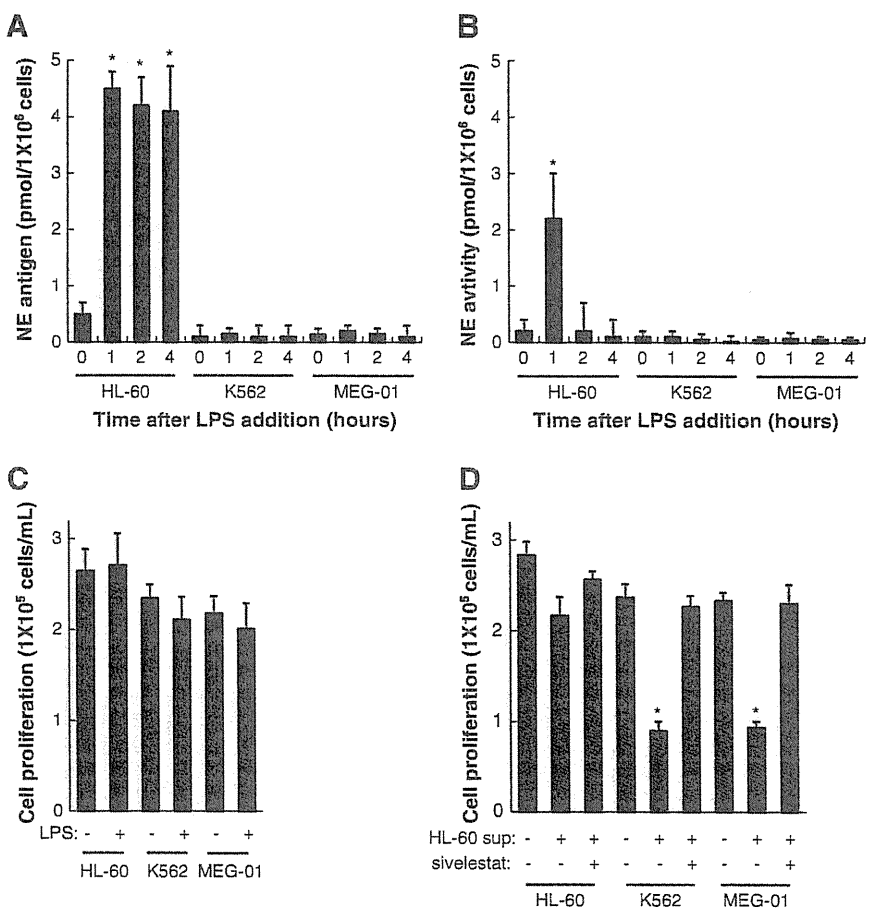

Fig. 1. Effects of LPS on secretion of neutrophil elastase and proliferation in hematological cells. A - B. 1×10^5 cells of three different hematological cell types HL-60, K562 and MEG-01 were stimulated with 10 ng/mL LPS for 0, 1, 2 and 4 hours. Neutrophil elastase antigen levels (A) and activity (B) were measured as described in the Materials and methods. C. 1×10^5 cells/mL HL-60, K562 and MEG-01 cells were cultured in the absence or presence of 10 ng/mL LPS. Cell numbers for each cell were counted at 24 hours by trypan-blue viable staining. D. 1×10^5 cells/mL of naïve HL-60, K562 and MEG-01 were cultured in the absence or presence of the supernatants derived from HL-60 cells that had been stimulated with 10 ng/mL LPS for 1 hour. HL-60, K562 and MEG-01 cells were also cultured in the presence of LPS-stimulated HL-60 supernatants treated with 100 nM sivelestat sodium. Cell numbers for each cell were counted at 24 hours. Values are mean ± SD; $^*p<0.03$ compared with controls. (A), (B) and (C) $n=5$, (D) $n=3$. NE, neutrophil elastase.

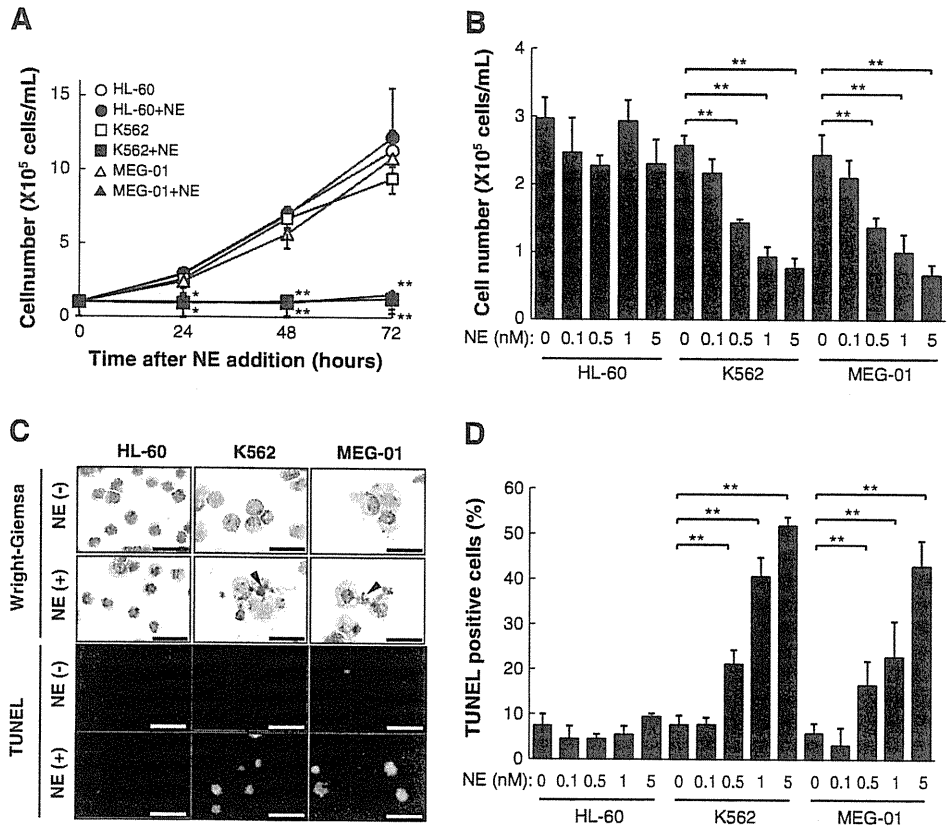

Fig. 2. Effects of neutrophil elastase on proliferation and induction of apoptosis in hematological cells. A. HL-60, K562 and MEG-01 cells were cultured in the absence or presence of 1 nM neutrophil elastase for 72 hours. Cell numbers for each cell were counted every 24 hours. B. HL-60, K562 and MEG-01 cells were cultured in the presence of 0–5 nM neutrophil elastase for 24 hours, and viable cell numbers were determined. C. Morphological changes in HL-60, K562 and MEG-01 cells were analyzed using Wright-Giemsa staining 24 hours post-stimulation with 1 nM neutrophil elastase (upper panels). For TUNEL labeling, apoptotic cells demonstrated a greater intensity of fluorescence (lower panels). Representative data from three independent experiments are shown. Arrow heads demonstrate apoptotic cells. Scale bars indicate 50 μm. D. The proportion of TUNEL-positive cells was calculated for each cell line treated with neutrophil elastase. Values are mean ± SD; $^{*}p<0.03$ and $^{**}p<0.01$ compared with controls. (A), and (B) $n=5$, (D) $n=3$. NE, neutrophil elastase.

HL-60 neutralizes neutrophil elastase activity by concomitant secretion of α1-antitrypsin

To clarify how HL-60 cells were not subject to apoptotic induction by neutrophil elastase, we measured residual antigen and enzymatic activity after its addition. We detected both antigen and enzymatic activity of neutrophil elastase in K562 and MEG-01 culture supernatants at levels similar to which they were added (Fig. 3 A and B). In HL-60 cultures, antigen levels of neutrophil elastase increased in a dose-dependent manner (Fig. 3 A), however enzymatic activity was not increased even after the addition of 0.3 or 1 nM neutrophil elastase (Fig. 3 B). Apoptotic effects on K562 and MEG-01 cultures were no longer evident when 1 nM neutrophil elastase was present together with its specific inhibitor, sivelestat sodium, at a concentration of 100 nM (Table 1), suggesting that cell type-specific apoptotic effects of neutrophil elastase might be based on its enzymatic activity. Thus, we focused on a natural inhibitor of neutrophil elastase, α1-antitrypsin. As shown in Fig. 3 C, HL-60 cells expressed α1-antitrypsin mRNAs, although the amount of mRNA did not increase after stimulation with neutrophil elastase. The α1-antitrypsin proteins were observed in the cytoplasmic granules of HL-60 cells but their appearance diminished following stimulation with neutrophil elastase (Fig. 3 D). Levels of α1-antitrypsin antigen in the culture medium of HL-60 cells significantly increased following stimulus with neutrophil elastase (Fig. 3 E). In contrast, α1-antitrypsin levels in HL-60 cell lysates were very low (Fig. 3 F).

Silencing of endogenous α1-antitrypsin expression with a shRNA lentiviral vector induces inhibition of HL-60 proliferation following the stimulation with neutrophil elastase

To confirm that the absence of α1-antitrypsin suppresses HL-60 growth when neutrophil elastase is present in the culture, we used siRNAs to knock down endogenous α1-antitrypsin expression. We examined the efficiency of the lentiviral shRNA for α1-antitrypsin with eGFP expression in HL-60 cells. As shown in Fig. 3 A, HL-60 cells transduced with the LentiLox-short hairpin or scramble α1-antitrypsin demonstrated expression of eGFP. Expression of α1-antitrypsin protein was significantly suppressed by transduction with LentiLox-short hairpin α1-antitrypsin (Fig. 4 B and C), demonstrating that silencing of endogenous α1-antitrypsin by a shRNA lentiviral vector system is effective in HL-60 cells. The proliferation of HL-60 cells transduced with the LentiLox-scramble α1-antitrypsin was not affected by neutrophil elastase (Fig. 4 D). However, α1-antitrypsin deficient HL-60 cells transduced with LentiLox-short hairpin sequences (Fig. 4 E) exhibited significant growth retardation after stimulation with neutrophil elastase (Fig. 4 D).

Effect of LPS on α1-antitrypsin deficient HL-60 cells transduced with a shRNA lentiviral vector

When HL-60 cells were stimulated with LPS, it was found that all cells secreted neutrophil elastase antigen regardless of whether they

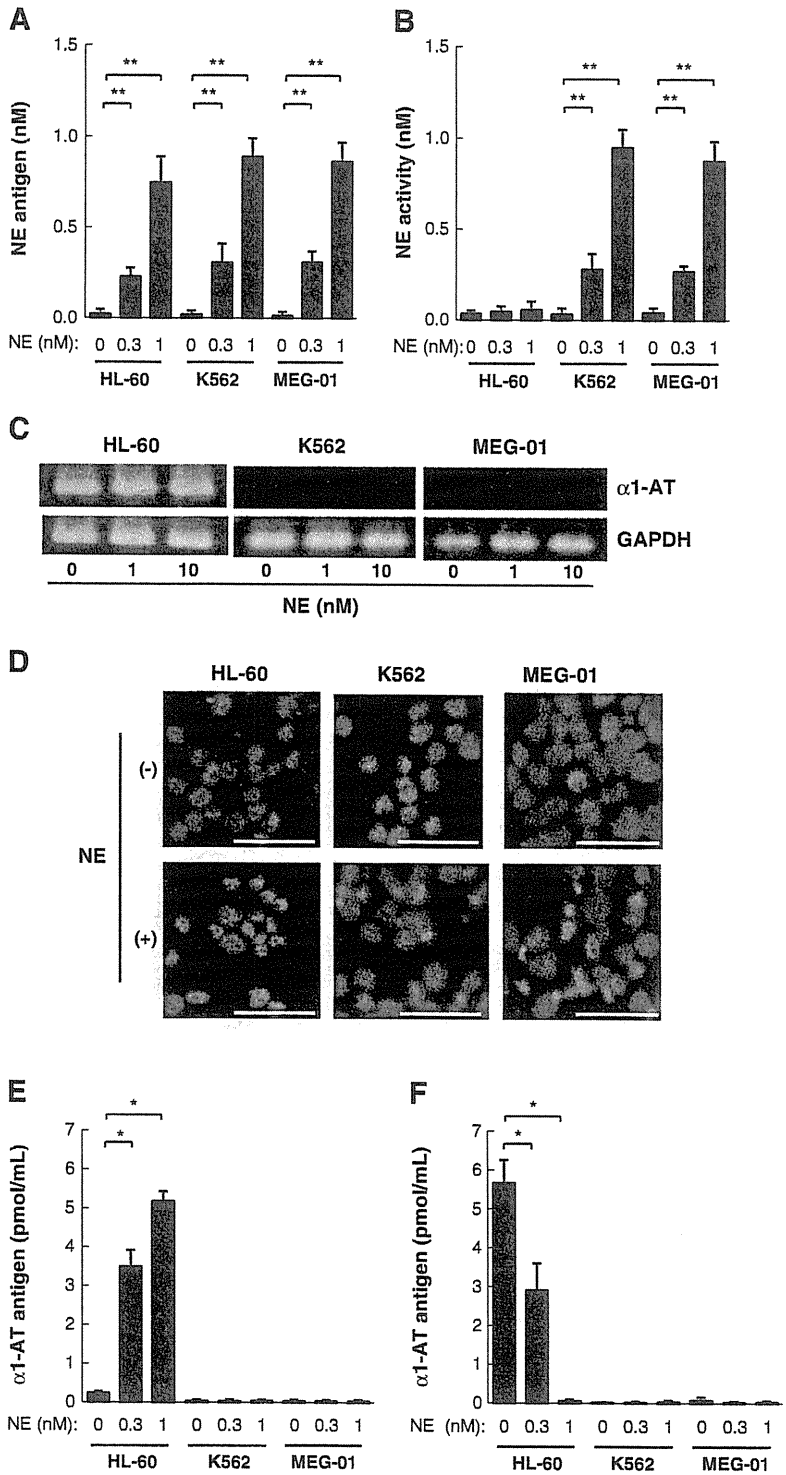

Fig. 3. HL-60 cells neutralize neutrophil elastase activity by secretion of α1-antitrypsin. A - B. Level of neutrophil elastase antigens (A) and enzyme activity (B) in a culture medium containing 1×10^5 cells/mL of HL-60, K562 and MEG-01 cells was measured 24 hours after the addition of neutrophil elastase (0, 0.3 and 1 nM), as described in the Materials and methods. C. HL-60, K562 and MEG-01 cells were cultured in the presence of 0–10 nM neutrophil elastase for 24 hours, and then α1-antitrypsin and GAPDH mRNA of each cell were analyzed by RT-PCR. D. HL-60, K562 and MEG-01 cells were cultured in the absence (upper panels) or presence (lower panels) of 1 nM neutrophil elastase for 24 hours, and then stained with anti-human α1-antitrypsin IgGs (red) and DAPI (blue) Scale bars indicate 50 μm. E-F. Levels of α1-antitrypsin antigens in culture medium (E) and cell lysate (F) of 1×10^5 cells/mL HL-60, K562 and MEG-01 cells were measured 24 hours after the addition of neutrophil elastase (0, 0.3 and 1 nM), as described in the Materials and methods. Values are the mean ± SD ($n = 3$, in each group). $^{**}p < 0.01$ compared with controls. NE, neutrophil elastase; α1-AT, α1-antitrypsin.

were transduced with LentiLox-scrambled or LentiLox-short hairpin α1-antitrypsin (Fig. 5 A). However, the neutrophil elastase activity in α1-antitrypsin deficient HL-60 cells was higher when compared to HL-60 controls or cells transduced with LentiLox-scrambled α1-antitrypsin (Fig. 5 B). Knock-down of α1-antitrypsin with the shRNA lentiviral vector efficiently suppressed α1-antitrypsin secretion

Table 1
Effect of sivelestat sodium on neutrophil elastase-induced apoptosis in hematological cells.

NE (nM)	sivelestat sodium (nM)	TUNEL positive cells (/1X103 cells)		
		HL-60	K562	MEG-01
0	0	4.7 ± 1.8	5.6 ± 1.9	3.0 ± 0.8
1	0	4.7 ± 0.6	47.2 ± 4.2**	39.8 ± 4.8**
1	10	4.2 ± 1.5	48.8 ± 5.4**	38.4 ± 2.5**
1	50	5.4 ± 2.3	34.7 ± 6.7**	28.0 ± 5.0**
1	100	4.4 ± 0.3	9.0 ± 2.2	7.7 ± 3.0

HL-60, K562 and MEG-01 cells were stimulated with 1 nM human neutrophil elastase in the presence of 0–100 nM of sivelestat sodium hydrate for 24 hours. TUNEL positive cells were calculated in each of 1×10^3 cells. Values are mean ± SD; n = 4; **$p < 0.01$ compared with controls. NE, neutrophil elastase.

following LPS-stimulus (Fig. 5 C). As expected, the growth of HL-60 cells transduced with LentiLox-short hairpin α1-antitrypsin was significantly suppressed when treated with LPS compared to cells transduced with LentiLox-scramble α1-antitrypsin (Fig. 5 D). Additionally, when HL-60 cells were stimulated with LPS in the presence of sivelestat sodium, levels of α1-antitrypsin in the culture medium did not increase (data not shown).

Effect of neutrophil elastase on in vitro differentiated hematological cells derived from CD34$^+$ progenitor cells

Human cord blood-derived CD34$^+$ progenitor cells were treated with differentiation protocols to produce cells of granulocytic, erythrocytic and megakaryocytic lineages as previously described [29]. We found that

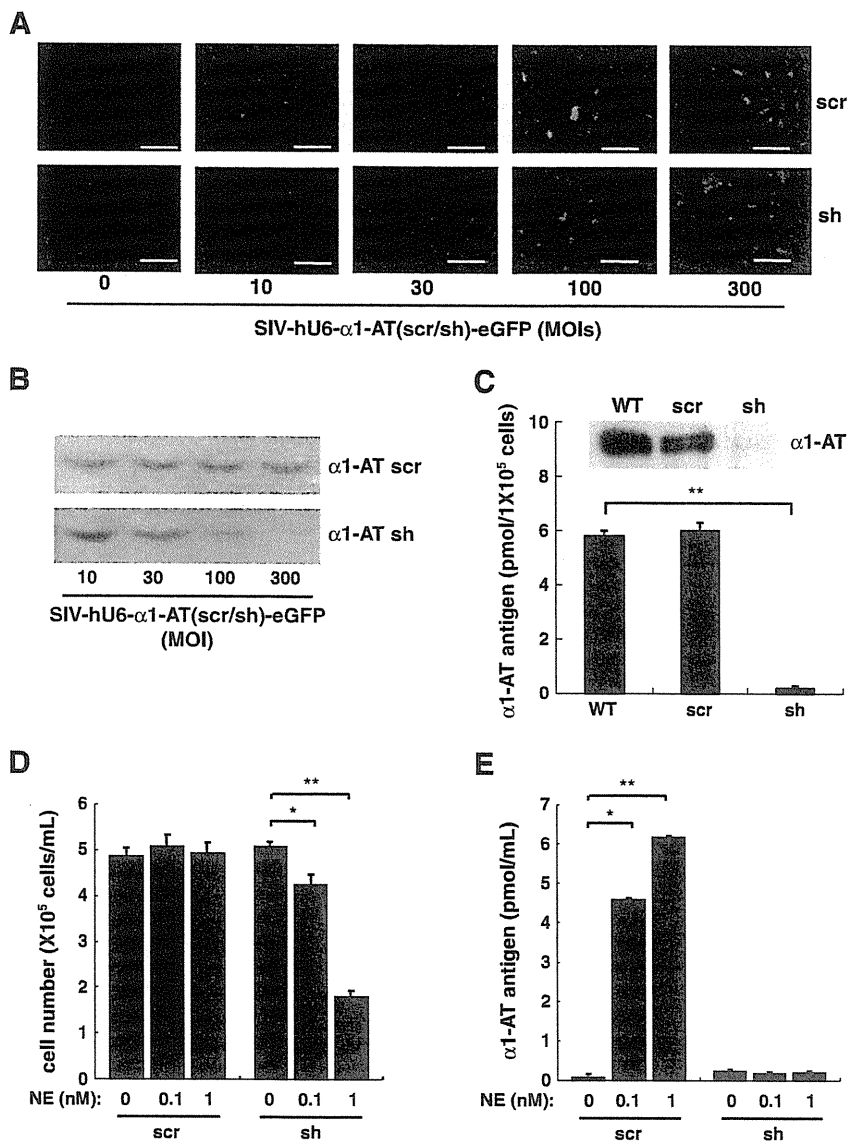

Fig. 4. Silencing of endogenous α1-antitrypsin expression with a shRNA lentiviral vector in HL-60 cells. A. HL-60 cells were transduced with LentiLox-scramble α1-antitrypsin (upper panels) or LentiLox-short hairpin α1-antitrypsin (lower panels) at multiplicities of infection (MOIs) of 0–300. Representative data from three independent experiments are shown. Scale bars show 50 μm. B. Cell lysates of HL-60 cells transduced with LentiLox vectors were analyzed with SDS-PAGE followed by Western blotting with anti-human α1-antitrypsin IgGs. Representative data from three independent experiments are shown. C. Amounts of α1-antitrypsin antigen were measured by ELISA in the cell lysates of 1×10^5 HL-60 cells transduced without (WT, $n = 5$) or with LentiLoxs (scr, $n = 5$; sh, $n = 5$). D - E. HL-60 cells transduced with LentiLox-short hairpin α1-antitrypsin or LentiLox-scramble α1-antitrypsin were cultured in the absence ($n = 5$) or presence of 0.1 nM ($n = 5$) and 1 nM ($n = 5$) neutrophil elastase for 72 hours and viable cell numbers (D) and antigen levels of α1-antitrypsin (E) were measured. Values are mean ± SD; *$p < 0.03$ and **$p < 0.01$ compared with controls. NE, neutrophil elastase; α1-AT, α1-antitrypsin; WT, non-transduced; scr, LentiLox-scramble α1-antitrypsin transduced; sh, LentiLox-short hairpin α1-antitrypsin transduced HL-60 cells.

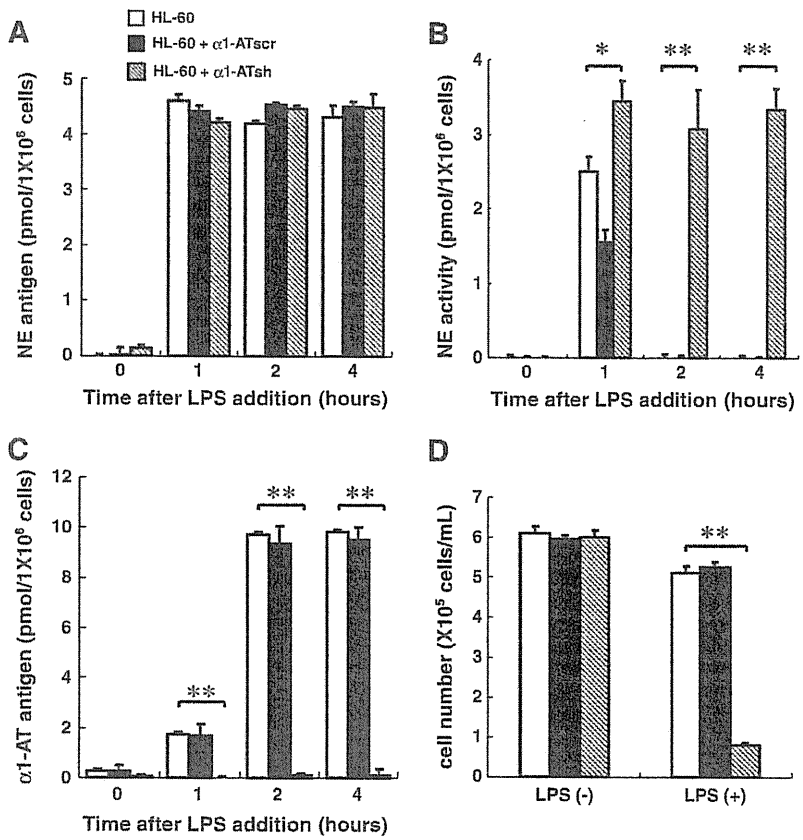

Fig. 5. Effects of LPS on α1-antitrypsin deficient HL-60 cells transduced with shRNA lentiviral vectors. A - C. 1×10^5 HL-60 cells ($n = 4$, bars), LentiLox-scramble transduced HL-60 cells ($n = 4$, shaded bars), LentiLox-short hairpin α1-antitrypsin transduced HL-60 cells ($n = 4$, hatched bars) were stimulated with 10 ng/mL LPS for 0, 1, 2 and 4 hours. Neutrophil elastase antigen levels (A), activity (B) and α1-antitrypsin antigen levels (C) were measured as described in the Materials and methods. D. 1×10^5 HL-60 cells ($n = 4$, bars), LentiLox-scramble transduced HL-60 cells ($n = 4$, shaded bars), LentiLox-short hairpin α1-antitrypsin transduced HL-60 cells ($n = 4$, hatched bars) were stimulated with 10 ng/mL LPS. After 48 hours, cell numbers of viable HL-60 cells were counted. Values are mean ± SD; $^*p < 0.03$ and $^{**}p < 0.01$ compared with controls. NE, neutrophil elastase; α1-AT, α1-antitrypsin; LPS, lipopolysaccharide.

progenitor cells could differentiate into three lineages, with the lineage of these cells determined by morphological assessment using a phase-contrast microscope, and detection of lineage-specific surface markers observed until 16 days after the induction of differentiation (Fig. 6 A). Interestingly, the only differentiated cells that concomitantly expressed neutrophil elastase with α1-antitrypsin mRNA were a granulocytic lineage, suggesting that this enzyme-inhibitor system may be up-regulated during granuloid cell differentiation. Proliferation of erythrocytic and megakaryocytic lineage cells was significantly suppressed by 1 nM neutrophil elastase as compared to granulocytic lineage cells (Fig. 6 D). Residual neutrophil elastase activity was found in erythrocytic as well as megakaryocytic cells with very little activity apparent in granulocytic cells (Fig. 6 E). However, only granulocytic lineage cells possessed α1-antitrypsin antigen in their culture supernatants after stimulation with neutrophil elastase (Fig. 6 F). We found that granulocytic lineage cells secreted significant amounts of active leukocyte elastase shortly after stimulation with LPS when compared to erythrocytic and megakaryocytic lineages (Fig. 6 B and C). When each lineage of cells was cultured with the supernatant derived from LPS-stimulated granulocytic cells, both erythrocytic and megakaryocytic lineage cells were significantly suppressed in their proliferation (Fig. 6 G).

Discussion

Neutrophil elastase is known to contribute towards combating bacterial infection [1–3]. Paradoxically, neutrophil elastase damages host tissues such as the intestine, kidney and lung during inflammation [10,30,31]. In our study, active neutrophil elastase was secreted not from K562 or MEG-01 but from HL-60 cells after stimulation of LPS (Fig. 1). In addition, the proliferation of K562 and MEG-01 was markedly inhibited after addition of culture medium derived from LPS-treated HL-60 cells, and the effects were canceled by sivelestat sodium. Several researchers have shown that neutrophil elastase induces endothelial and epithelial apoptosis [10,32]. We showed that neutrophil elastase significantly inhibited proliferation of K562 as well as MEG-01 cells by inducing apoptosis (Fig. 2). Interestingly, neutrophil elastase did not affect cell growth of HL-60 cells. Thus, the damage of hematological cells may involve a disturbance in the balance between neutrophil elastase activity and its inhibitor in response to LPS.

It has been reported that neutrophils respond to surface stimulation by secreting neutrophil elastase and α1-antitrypsin, and that there might be an inherent mechanism for damping the local effects of neutrophil elastase [33,34]. Apoptotic effects of neutrophil elastase on K562 and MEG-01 cultures were absent when the enzymatic activity of neutrophil elastase was neutralized by sivelestat sodium (Table 1) [31,35]. Only HL-60 cells exhibited resistance to apoptotic induction as they stored α1-antitrypsin, which was secreted rapidly after stimulation by neutrophil elastase (Fig. 3). These results suggest that cell type-specific effects of neutrophil elastase on hematological cell growth might be dependent on the neutralizing activity of neutrophil elastase by endogenous α1-antitrypsin.

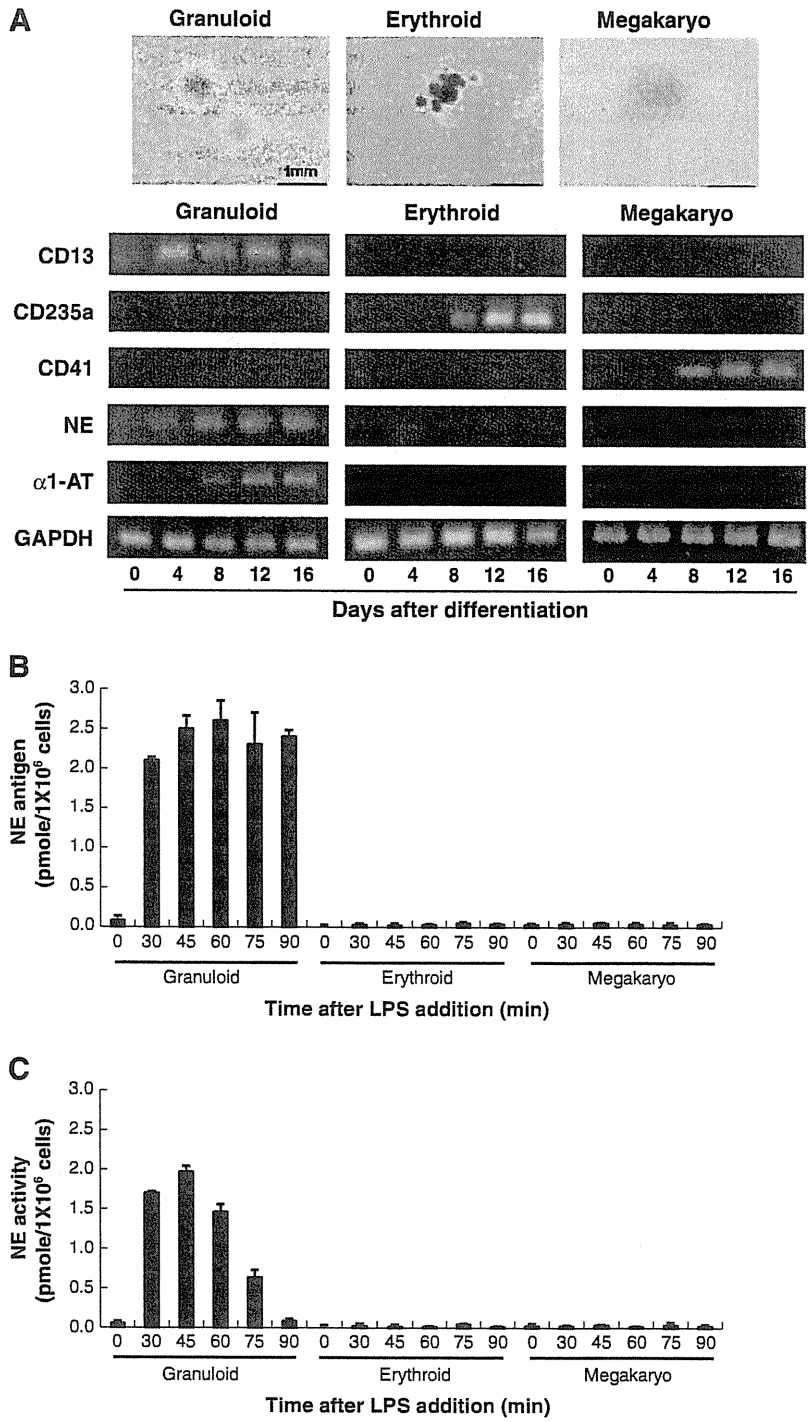

Fig. 6. *In vitro* differentiation of cord blood-derived $CD34^+$ progenitor cells towards three lineages of hematological cells and their responses against LPS or neutrophil elastase. A. Human cord blood-derived $CD34^+$ progenitor cells were differentiated *in vitro* into granulocytic cells (left panels), erythrocytic cells (middle panels) and megakaryocytic cells (right panels) as described in the Materials and Methods. Each cell type was harvested at the indicated time points, and subjected to RT-PCR analysis for CD13, CD235a, CD41, neutrophil elastase (NE), α1-antitrypsin (α1-AT) and GAPDH mRNA expression. Representative data from three independent experiments are shown. B - C. 1×10^5 differentiated granulocytic, erythrocytic and megakaryocytic cells were stimulated with 10 ng/mL LPS for 0–90 minutes. Neutrophil elatastase antigen levels (B) and activity (C) were measured as described in Materials and methods. D. Differentiated granulocytic (circles), erythrocytic (filled circles) and megakaryocytic cells (triangles) were cultured in the presence of 1 nM neutrophil elastase for 72 hours. Cell numbers were determined every 24 hours. E - F. 1×10^5 differentiated cells were cultured with 0, 0.3 and 1 nM neutrophil elastase for 24 hours and neutrophil elastase acitvity (E) and α1-antitrypsin antigen levels (F) were measured. 1×10^5 differentiated granulocytic cells were also cultured for 24 hours in the presence of 1 nM neutrophil elastase that had been treated with 100 nM sivelestat sodium, and neutrophil elastase activity was measured (E). G. Differentiated granulocytic (circles), erythrocytic (filled circles) and megakaryocytic cells (triangles) were cultured for 72 hours in the presence of granulocytic cell-derived culture medium that had been stimulated with 10 ng/mL LPS for 45 minutes. Viable cell numbers were determined every 24 hours. The values given are the mean ± SD; $n = 4$; $^*p<0.03$ and $^{**}p<0.01$ compared with controls.

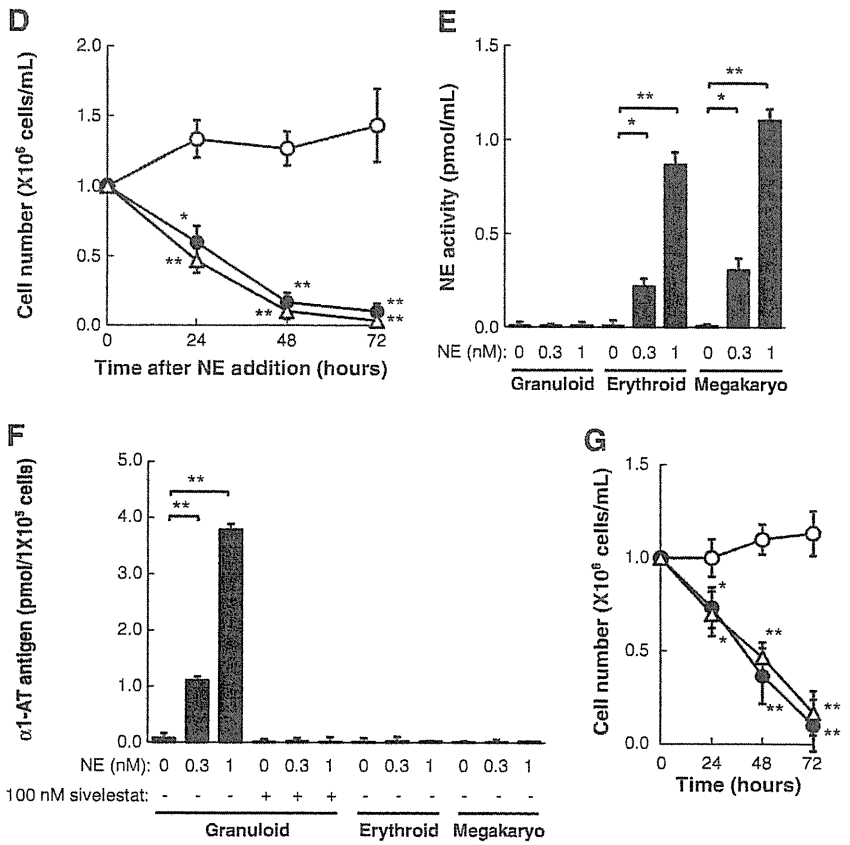

Fig. 6 (*continued*).

Leukocyte are known to release neutrophil elastase as well as α1-antitrypisn in response to LPS [28,36]. In our study, silencing of α1-antitrypsin expression with a short hairpin RNA lentiviral vector inhibited growth of HL-60 cells in the presence of neutrophil elastase (Fig. 4). In addition, HL-60 cells transduced with LentiLox-scrambled and -short hairpin α1-antitrypsin sequences secreted significant amounts of neutrophil elastase proteins shortly after stimulation with LPS (Fig. 5). The enzymatic activity of neutrophil elastase was only found in HL-60 cultures that had been transduced with LentiLox-short hairpin α1-antitrypsin which resulted in a significant reduction in cell growth. Moreover, K562 and MEG-01 cells did not express neutrophil elastase after LPS stimulation, and their proliferation was not significantly suppressed by LPS (Fig. 1). Taken together, our data suggests that LPS might stimulate secretion of neutrophil elastase, resulting in induction of neutrophil elastase-mediated apoptosis if its enzymatic activity is not efficiently neutralized by released α1-antitrypsin.

Although the cell surface receptor involved in neutrophil elastase has not been clearly identified, several candidates are suggested, such as protease-activated receptor (PAR)-2 and Toll-like receptor (TLR)-4 [8,37,38]. Additionally, the apoptosis induced by neutrophil elastase might be mediated through PAR-1 [39]. TLR-4 appears to be the principle receptor for LPS and mediates the activation of nuclear factor κB as well as the synthesis of proinflammatory cytokines such as interleukin-8 [8,40]. Tsujimoto *et al* showed that neutrophil elastase might be associated with expression of TLR-4 on monocytes and macrophages in the septic state [41]. In our study, TLR-4 was expressed in K562, MEG-01 and HL-60 cells [42], however, none of these hematological cells expressed PAR-1 or PAR-2 (data not shown), suggesting that the neutrophil elastase-induced apoptosis may be mediated through a signaling pathway similar to that for TLR-4.

Our *in vitro* differentiation models of hematopoiesis using $CD34^+$ progenitor cells showed that only granulocytic lineage cells expressed neutrophil elastase (Fig. 6), which is consistent with previous studies where levels of neutrophil elastase expression reach a maximum in the promyelocyte and are maintained until differentiation into a neutrophil [43,44]. Importantly, α1-antitrypsin was concomitantly expressed with neutrophil elastase during differentiation into a granulocytic lineage [34,45]. Additionally, α1-antitrypsin was secreted after stimulation by neutrophil elastase, and neutralized it to prevent growth inhibition. When we added inactive neutrophil elastase pretreated with sivelestat sodium to granulocytic lineage cells, we could not detect any α1-antitrypsin antigen (Fig. 6), suggesting that the enzymatic activity of neutrophil elastase might be crucial in secreting α1-antitrypsin. El Ouriaghli and coworkers reported that neutrophil elastase inhibits proliferation and induces apoptosis in $CD34^+$ cells along with degradation of G-CSF [17]. Although our *in vitro* hematopoietic differentiation system was free from G-CSF, concurrently secreted α1-antitrypsin may regulate neutrophil elastase activity. Granulocytic lineage cells released neutrophil elastase following stimulation with LPS, and active neutrophil elastase was neutralized for 90 minutes (Fig. 6). LPS stimulation did not affect erythrocytic or megakaryocytic lineage cells, however, the supernatant derived from granulocytic lineage cells 45 minutes after the addition of LPS significantly inhibited their proliferation as they could not inactivate neutrophil elastase. Erythropoiesis and megakaryopoiesis may be inhibited by neutrophil elastase due to the absence of α1-antitrypsin in these lineages in the inflammatory state. Thus, α1-antitrypsin released from granulocytes might play an important role for the maintenance of hematopoiesis in microenvironments such as the bone marrow niche where α1-antitrypsin might not be sufficiently supplied from plasma [36,46].

In conclusion, we demonstrated that hematological cells might be affected by neutrophil elastase which is regulated by endogenous α1-antitrypsin under the stimulation of lipopolysaccharide. We suggest that granulocytes could protect themselves from neutrophil elastase-induced cellular damage by efficiently neutralizing its activity with concomitant secretion of endogenous α1-antitrypsin. Extensive clinical studies would be required for understanding the precise mechanism of controlling neutrophil elastase activity by endogenous α1-antitrypsin in septic patients.

Authorship contribution

M. Dokai and S. Madoiwa designed and performed the research, analyzed the data, and wrote the paper; A. Yasumoto, Y. Kashiwakura, A. Ishiwata, A. Sakata and N. Makino performed experiments; S. Madoiwa, T. Ohmori, J. Mimuro, and Y. Sakata analyzed data and revised the paper.

Disclosure of conflicts of interest

The authors state that they have no conflict of interest to declare.

Acknowledgements

We thank D.V.M. Hisae Yamauchi, D.V.M. Akane Hirasawa and Ms. Chizuko Nakamikawa for their technical assistance. This work was supported in part by a Grant-in-Aid for Scientific Research (#19591133, #20591155, #21790920 and #21591249) from the Ministry of Education, Culture, Sports, Science and Technology, and by a Health and Labor Sciences Research Grant for Research from the Ministry of Health, Labor and Welfare, also by a Support Program for Strategic Research Platform, and using JKA promotion funds from KEIRIN RACE.

References

[1] Belaaouaj A, McCarthy R, Baumann M, Gao Z, Ley TJ, Abraham SN, et al. Mice lacking neutrophil elastase reveal impaired host defense against gram negative bacterial sepsis. Nat Med 1998;4:615–8.
[2] Belaaouaj A, Kim KS, Shapiro SD. Degradation of outer membrane protein A in Escherichia coli killing by neutrophil elastase. Science 2000;289:1185–8.
[3] Reeves EP, Lu H, Jacobs HL, Messina CG, Bolsover S, Gabella G, et al. Killing activity of neutrophils is mediated through activation of proteases by K+flux. Nature 2002;416:291–7.
[4] Weinrauch Y, Drujan D, Shapiro SD, Weiss J, Zychlinsky A. Neutrophil elastase targets virulence factors of enterobacteria. Nature 2002;417:91–4.
[5] Janoff A. Elastase in tissue injury. Annu Rev Med 1985;36:207–16.
[6] Sinha S, Watorek W, Karr S, Giles J, Bode W, Travis J. Primary structure of human neutrophil elastase. Proc Natl Acad Sci USA 1987;84:2228–32.
[7] Ono T, Mimuro J, Madoiwa S, Soejima K, Kashiwakura Y, Ishiwata A, et al. Severe secondary deficiency of von Willebrand factor-cleaving protease (ADAMTS13) in patients with sepsis-induced disseminated intravascular coagulation: its correlation with development of renal failure. Blood 2006;107:528–34.
[8] Devaney JM, Greene CM, Taggart CC, Carroll TP, O'Neill SJ, McElvaney NG. Neutrophil elastase up-regulates interleukin-8 via toll-like receptor 4. FEBS Lett 2003;544:129–32.
[9] Perlmutter DH, Travis J, Punsal PI. Elastase regulates the synthesis of its inhibitor, alpha 1-proteinase inhibitor, and exaggerates the defect in homozygous PiZZ alpha 1 PI deficiency. J Clin Invest 1988;81:1774–80.
[10] Ginzberg HH, Shannon PT, Suzuki T, Hong O, Vachon E, Moraes T, et al. Leukocyte elastase induces epithelial apoptosis: role of mitochondial permeability changes and Akt. Am J Physiol Gastrointest Liver Physiol 2004;287:G286–98.
[11] Fischer BM, Cuellar JG, Byrd AS, Rice AB, Bonner JC, Martin LD, et al. ErbB2 activity is required for airway epithelial repair following neutrophil elastase exposure. FASEB J 2005;19:1374–6.
[12] Crystal RG, Brantly ML, Hubbard RC, Curiel DT, States DJ, Holmes MD. The alpha 1-antitrypsin gene and its mutations. Clinical consequences and strategies for therapy. Chest 1989;95:196–208.
[13] Lomas DA, Evans DL, Finch JT, Carrell RW. The mechanism of Z alpha 1-antitrypsin accumulation in the liver. Nature 1992;357:605–7.
[14] Turino GM, Seniorrm, Garg BD, Keller S, Levi MM, Mandl I. Serum elastase inhibitor deficiency and alpha 1-antitrypsin deficiency in patients with obstructive emphysema. Science 1969;165:709–11.
[15] Stoller JK, Aboussouan LS. Alpha1-antitrypsin deficiency. Lancet 2005;365:2225–36.
[16] Gross B, Grebe M, Wencker M, Stoller JK, Bjursten LM, Janciauskiene S. New Findings in PiZZ alpha1-antitrypsin deficiency-related panniculitis. Demonstration of skin polymers and high dosing requirements of intravenous augmentation therapy. Dermatology 2009;218:370–5.
[17] El Ouriaghli F, Fujiwara H, Melenhorst JJ, Sconocchia G, Hensel N, Barrett AJ. Neutrophil elastase enzymatically antagonizes the in vitro action of G-CSF: implications for the regulation of granulopoiesis. Blood 2003;101:1752–8.
[18] Horwitz M, Benson KF, Person RE, Aprikyan AG, Dale DC. Mutations in ELA2, encoding neutrophil elastase, define a 21-day biological clock in cyclic haematopoiesis. Nat Genet 1999;23:433–6.
[19] Li FQ, Horwitz M. Characterization of mutant neutrophil elastase in severe congenital neutropenia. J Biol Chem 2001;276:14230–41.
[20] Horwitz MS, Duan Z, Korkmaz B, Lee HH, Mealiffe ME, Salipante SJ. Neutrophil elastase in cyclic and severe congenital neutropenia. Blood 2007;109:1817–24.
[21] Goselink HM, Hiemstra PS, van Noort P, Barge RM, Willemze R, Falkenburg JH. Cytokine-dependent proliferation of human CD34+ progenitor cells in the absence of serum is suppressed by their progeny's production of serine proteinases. Stem Cells 2006;24:299–306.
[22] Fonseca RB, Mohr AM, Wang L, Sifri ZC, Rameshwar P, Livingston DH. The impact of a hypercatecholamine state on erythropoiesis following severe injury and the role of IL-6. J Trauma 2005;59:884–9 discussion 9–90.
[23] Livingston DH, Anjaria D, Wu J, Hauser CJ, Chang V, Deitch EA, et al. Bone marrow failure following severe injury in humans. Ann Surg 2003;238:748–53.
[24] Suehiro Y, Muta K, Nakashima M, Abe Y, Shiratsuchi M, Shiokawa S, et al. A novel mechanism in suppression of erythropoiesis during inflammation: a crucial role of RCAS1. Eur J Haematol 2005;74:365–73.
[25] Chandra R, Villanueva E, Feketova E, Machiedo GW, Hasko G, Deitch EA, et al. Endotoxemia down-regulates bone marrow lymphopoiesis but stimulates myelopoiesis: the effect of G6PD deficiency. J Leukoc Biol 2008;83:1541–50.
[26] Madoiwa S, Komatsu N, Mimuro J, Kimura K, Matsuda M, Sakata Y. Developmental expression of plasminogen activator inhibitor-1 associated with thrombopoietin-dependent megakaryocytic differentiation. Blood 1999;94:475–82.
[27] Oltmanns U, Sukkar MB, Xie S, John M, Chung KF. Induction of human airway smooth muscle apoptosis by neutrophils and neutrophil elastase. Am J Respir Cell Mol Biol 2005;32:334–41.
[28] Ottonello L, Barbera P, Dapino P, Sacchetti C, Dallegri F. Chemoattractant-induced release of elastase by lipopolysaccharide (LPS)-primed neutrophils; inhibitory effect of the anti-inflammatory drug nimesulide. Clin Exp Immunol 1997;110:139–43.
[29] Miller C, B. L. Human and mouse hematopoietic colony-forming cell assays. Basic Cell Culture Protocols 3. Methods Mol Biol 2005;290:71–89.
[30] Lee WL, Downey GP. Leukocyte elastase: physiological functions and role in acute lung injury. Am J Respir Crit Care Med 2001;164:896–904.
[31] Zeiher BG, Matsuoka S, Kawabata K, Repine JE. Neutrophil elastase and acute lung injury: prospects for sivelestat and other neutrophil elastase inhibitors as therapeutics. Crit Care Med 2002;30:S281–7.
[32] Yang JJ, Kettritz R, Falk RJ, Jennette JC, Gaido ML. Apoptosis of endothelial cells induced by the neutrophil serine proteases proteinase 3 and elastase. Am J Pathol 1996;149:1617–26.
[33] du Bois RM, Bernaudin JF, Paakko P, Hubbard R, Takahashi H, Ferrans V, et al. Human neutrophils express the alpha 1-antitrypsin gene and produce alpha 1-antitrypsin. Blood 1991;77:2724–30.
[34] Paakko P, Kirby M, du Bois RM, Gillissen A, Ferrans VJ, Crystal RG. Activated neutrophils secrete stored alpha 1-antitrypsin. Am J Respir Crit Care Med 1996;154:1829–33.
[35] Hagiwara S, Iwasaka H, Hidaka S, Hasegawa A, Noguchi T. Neutrophil elastase inhibitor (sivelestat) reduces the Levels of inflammatory mediators by inhibiting NF-kB. Inflamm Res 2009;58:1–6.
[36] Knoell DL, Ralston DR, Coulter KR, Wewers MD. Alpha 1-antitrypsin and protease complexation is induced by lipopolysaccharide, interleukin-1beta, and tumor necrosis factor-alpha in monocytes. Am J Respir Crit Care Med 1998;157:246–55.
[37] Uehara A, Muramoto K, Takada H, Sugawara S. Neutrophil serine proteinases activate human nonepithelial cells to produce inflammatory cytokines through protease-activated receptor 2. J Immunol 2003;170:5690–6.
[38] Walsh DE, Greene CM, Carroll TP, Taggart CC, Gallagher PM, O'Neill SJ, et al. Interleukin-8 up-regulation by neutrophil elastase is mediated by MyD88/IRAK/TRAF-6 in human bronchial epithelium. J Biol Chem 2001;276:35494–9.
[39] Suzuki T, Moraes TJ, Vachon E, Ginzberg HH, Huang TT, Matthay MA, et al. Proteinase-activated receptor-1 mediates elastase-induced apoptosis of human lung epithelial cells. Am J Respir Cell Mol Biol 2005;33:231–47.
[40] Williams DL, Ha T, Li C, Kalbfleisch JH, Schweitzer J, Vogt W, et al. Modulation of tissue Toll-like receptor 2 and 4 during the early phases of polymicrobial sepsis correlates with mortality. Crit Care Med 2003;31:1808–18.
[41] Tsujimoto H, Ono S, Majima T, Kawarabayashi N, Takayama E, Kinoshita M, et al. Neutrophil elastase, MIP-2, and TLR-4 expression during human and experimental sepsis. Shock 2005;23:39–44.
[42] Mita Y, Dobashi K, Nakazawa T, Mori M. Induction of Toll-like receptor 4 in granulocytic and monocytic cells differentiated from HL-60 cells. Br J Haematol 2001;112:1041–7.
[43] Takahashi H, Nukiwa T, Basset P, Crystal RG. Myelomonocytic cell lineage expression of the neutrophil elastase gene. J Biol Chem 1988;263:2543–7.
[44] Fouret P, du Bois RM, Bernaudin JF, Takahashi H, Ferrans VJ, Crystal RG. Expression of the neutrophil elastase gene during human bone marrow cell differentiation. J Exp Med 1989;169:833–45.
[45] Joslin G, Griffin GL, August AM, Adams S, Fallon RJ, Senior RM, et al. The serpin-enzyme complex (SEC) receptor mediates the neutrophil chemotactic effect of alpha-1 antitrypsin-elastase complexes and amyloid-beta peptide. J Clin Invest 1992;90:1150–4.
[46] Arai F, Hirao A, Ohmura M, Sato H, Matsuoka S, Takubo K, et al. Tie2/angiopoietin-1 signaling regulates hematopoietic stem cell quiescence in the bone marrow niche. Cell 2004;118:149–61.

Recovery of neurogenic amines in phenylketonuria mice after liver-targeted gene therapy

Hiroya Yagi[a,b], Sho Sanechika[c], Hiroshi Ichinose[c], Chiho Sumi-Ichinose[d], Hiroaki Mizukami[a], Masashi Urabe[a], Keiya Ozawa[a] and Akihiro Kume[a]

Phenylketonuria (PKU) is a common genetic disorder arising from a deficiency of phenylalanine hydroxylase. If left untreated, the accumulation of phenylalanine leads to brain damage and neuropsychological dysfunction. One of the abnormalities found in hyperphenylalaninemic patients and a mouse model of PKU is an aminergic deficit in the brain. We previously showed correction of hyperphenylalaninemia and concomitant behavioral recovery in PKU mice after liver-targeted gene transfer with a viral vector. Here, we addressed whether such a functional recovery was substantiated by an improved amine metabolism in the brain. After gene transfer, brain dopamine, norepinephrine, and serotonin levels in the PKU mice were significantly elevated to normal or near-normal levels, along with systemic improvement of phenylalanine catabolism. The results of biochemical analyses validated the efficacy of PKU gene therapy in the central nervous system. *NeuroReport* **23:30–34 © 2011 Wolters Kluwer Health | Lippincott Williams & Wilkins.**

NeuroReport 2012, 23:30–34

Keywords: catecholamine, gene therapy, phenylketonuria, serotonin

[a]Division of Genetic Therapeutics, Jichi Medical University, Shimotsuke, [b]Department of Obstetrics and Gynecology, Institute of Clinical Medicine, University of Tsukuba, Tsukuba, [c]Department of Life Science, Graduate School of Bioscience and Biotechnology, Tokyo Institute of Technology, Yokohama and [d]Department of Pharmacology, School of Medicine, Fujita Health University, Toyoake, Japan

Correspondence to Dr Akihiro Kume, MD, PhD, Division of Genetic Therapeutics, Jichi Medical University, 3311-1 Yakushiji, Shimotsuke, Tochigi 329-0498, Japan Tel: +81 285 58 7402; fax: +81 285 44 8675; e-mail: kume@jichi.ac.jp

Received 1 September 2011 accepted 17 October 2011

Introduction

Phenylketonuria (PKU; OMIM 261600) is a common inherited metabolic disorder, mostly arising from a deficiency of phenylalanine hydroxylase (PAH) [1]. PAH is exclusively responsible for converting phenylalanine into tyrosine, and its deficiency results in a systemic accumulation of phenylalanine in the body. Although the mechanisms involved are not fully understood, excessive amounts of phenylalanine are toxic to the developing brain and have a negative impact on neuropsychological function in adults. Therefore, the present treatment for PKU mandates strict restrictions of dietary protein in infancy and childhood to limit phenylalanine intake, and a similar diet is recommended for life. One possible mechanism responsible for the neurological dysfunction is an aminergic deficit, as earlier studies showed drastic decreases in neurotransmitters such as dopamine, norepinephrine, and serotonin (5-hydroxytryptamine, 5-HT) in the brains of untreated PKU patients [2,3]. A similar aminergic deficit was found in a mouse model of PKU (the *Pah*^{enu2} strain) [4–7]. We and other investigators have explored the feasibility of somatic gene therapy for PKU, and have shown that recombinant adeno-associated virus (AAV) vectors can achieve long-term corrections of hyperphenylalaninemia (HPA) in *Pah*^{enu2} mice [8–10]. We also demonstrated a behavioral recovery in the treated animals, indicating that some brain functions benefited from this approach [8]. In the present study, we addressed whether liver-targeted gene therapy for PKU would reinstate the metabolism of neurogenic amines, thereby improving homeostasis and the function of the central nervous system.

Materials and methods

Animals

All the animal experiments were carried out in accordance with the institutional guidelines under protocols approved by the Institutional Animal Care and Use Committee at Jichi Medical University (Shimotsuke, Japan). PAH-deficient C57BL/6-*Pah*^{enu2} mice (PKU mice, −/−) were homozygous for the same *Pah*^{enu2} mutation as that described in the original BTBR-*Pah*^{enu2} strain [4,5], but had been bred and backcrossed on the C57BL/6J background. Genotyping for the presence of the *Pah*^{enu2} mutation was performed by PCR analysis of tail biopsy DNA [9]. All the mice were maintained on standard mouse chow (CE-2 from Clea, Tokyo, Japan). Blood was collected from the tail veins on a filter paper for newborn mass screening (No. 545 from Advantec Toyo, Tokyo, Japan), and blood phenylalanine concentrations were determined by an enzymatic fluorometric assay using an Enzaplate PKU-R kit (GE Healthcare, Tokyo, Japan) and a Fluoroskan Ascent FL plate reader (Labsystems, Helsinki, Finland) [8,9]. *In-vivo* phenylalanine oxidation was evaluated by a noninvasive breath test using [1-^{13}C]L-phenylalanine [9,11].

In-vivo gene transfer

The construction and preparation of the AAV8-pseudotyped self-complementary AAV vector for PKU (scAAV8/

0959-4965 © 2011 Wolters Kluwer Health | Lippincott Williams & Wilkins

DOI: 10.1097/WNR.0b013e32834e3a87

LP1-mPAH) has been described previously [9]. 1×10^{11} vector genomes of the recombinant AAV were dissolved in 0.5 ml of saline and injected into the peritoneal cavity of a PKU mouse at 8 weeks of age.

Brain sampling and biochemical analysis

Mice were killed by cervical dislocation, and the removed brain was immediately frozen in liquid nitrogen and stored at −80°C until used. The brain was homogenized in 10 volumes of 0.2 M of perchloric acid containing 0.1 mM of EDTA for deproteination. Protein concentrations were determined using a DC protein assay kit (Bio-Rad, Hercules, California, USA). Catecholamine and 5-HT levels were measured by high-performance liquid chromatography using an electrochemical detector ECD-100 (EICOM, Kyoto, Japan) as described elsewhere [12]. Amino acid levels were analyzed using an L-8500 amino acid analyzer (Hitachi, Tokyo, Japan). Data are presented as means ± SDs in the text and figures. An unpaired *t*-test was performed using the StatView 5.0 software for Macintosh (SAS Institute, Cary, North Carolina, USA) for comparison between two groups, and a *P* value of less than 0.05 was considered to be significant.

Results

Phenotypic correction after gene transfer

As shown in the original BTBR-*Pah*^{enu2} mice [9], the scAAV8/LP1-mPAH vector exhibited remarkable efficacy in restoring phenylalanine catabolism in C57BL/6-*Pah*^{enu2} mice. Before the gene transfer, PKU mice had elevated blood phenylalanine levels (28.1 ± 1.7 mg/dl; $n = 3$) compared with their heterozygous (+/−) littermates (0.3 ± 0.2 mg/dl; $n = 6$), whereas blood phenylalanine levels in heterozygous mice were indistinguishable from those in wild-type homozygous (WT, +/+) mice (0.3 ± 0.1 mg/dl; $n = 6$). After a single injection of the AAV vector to PKU mice, the blood phenylalanine concentration rapidly decreased to a near-normal level in 1 week (1.7 ± 0.8 mg/dl) and remained within the normal range from weeks 2 to 8 (Fig. 1a). In parallel, we evaluated phenylalanine-oxidizing capacity by conducting a ^{13}C-phenylalanine-loading breath test (Fig. 1b). In this assay, the production of $^{13}CO_2$ (ΔCO_2) is associated with PAH activity, although we were not able to distinguish heterozygous mice (50.6 ± 6.7‰; $n = 6$) from WT mice (52.6 ± 10.5‰; $n = 6$), presumably due to other limiting factors such as phenylalanine transport and cofactor availability *in vivo*. Before the gene transfer, PKU mice produced very little, if any, ΔCO_2 (2.0 ± 1.1‰; $n = 3$). One week post-AAV injection, ΔCO_2 was increased to 2/3 of the control level (29.9 ± 1.1‰) and the value gradually increased to a near-normal level (41.8 ± 3.5‰ at week 8).

The AAV-treated PKU mice ($n = 3$) were euthanized at week 8 after injection along with heterozygous littermates ($n = 6$) and age-matched, untreated PKU mice ($n = 4$) for further analysis. First, we measured the whole brain weight of these animals (Fig. 1c). As reported [13], the weight of the brain in untreated PKU mice was significantly decreased compared with the control level (343 ± 15 vs. 481 ± 33 mg; $P = 0.00005$). In contrast, the brains of AAV-treated PKU animals regained weight significantly (431 ± 26 mg; $P = 0.0023$ vs. untreated PKU), reaching a level comparable level to that in heterozygous mice ($P = 0.55$).

Amino acid analysis

In the amino acid analysis, we confirmed that the untreated PKU mice had a marked imbalance of phenylalanine and tyrosine in the brain [13] (Fig. 2a). The phenylalanine content was nearly 10 times that of heterozygous mice (6.24 ± 0.81 vs. 0.66 ± 0.08 nmol/mg protein; $P = 0.0008$), whereas the tyrosine content was lower (0.31 ± 0.08 vs. 0.77 ± 0.09 nmol/mg protein; $P = 0.0005$). In the AAV-treated PKU mice, the amount of phenylalanine in the

Fig. 1

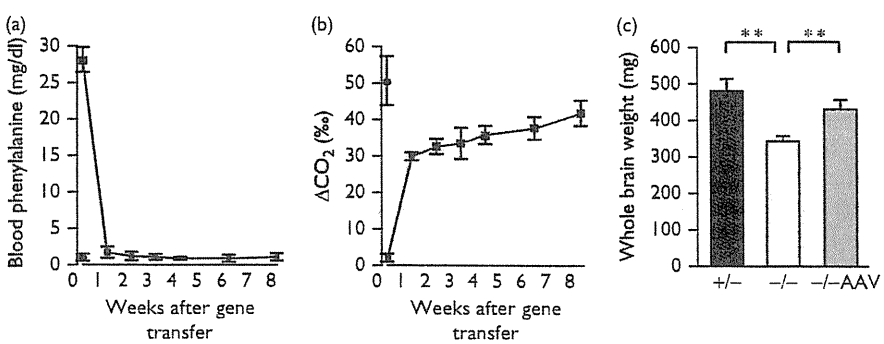

Phenotypic correction in phenylketonuria (PKU) mice after gene transfer. (a) Blood phenylalanine levels in adeno-associated virus (AAV)-treated PKU mice (squares) and heterozygous controls (circle). (b) $^{13}CO_2$ production (ΔCO_2) by AAV-treated PKU mice (squares) and heterozygous controls (circle) in a [1-^{13}C]L-phenylalanine-loading test. (c) Whole brain weights of heterozygous control (+/−), untreated PKU (−/−), and AAV-treated PKU (−/− AAV) mice. Data are shown as the mean ± SD. **$P < 0.01$.

brain was decreased (1.04 ± 0.50 nmol/mg of protein; $P = 0.001$ vs. untreated PKU) in accordance with that in blood. The treated mice also had increased levels of tyrosine, but the elevation was not significant because one animal had a supranormal tyrosine content (1.55 nmol/mg of protein) that resulted in a relatively large SD for this group. As for tryptophan, the untreated PKU mice had a lower average level (0.12 ± 0.05 nmol/mg protein) than the heterozygous and AAV-treated mice (0.21 ± 0.11 and 0.28 ± 0.13 nmol/mg of protein, respectively), but the difference was not significant as reported previously [7].

Monoamine neurotransmitters and metabolites

The levels of catecholamines, serotonin, and metabolites are summarized in Table 1. We confirmed that the amounts of dopamine, norepinephrine, and 5-HT in the untreated PKU mice were significantly decreased compared with those in the heterozygous controls ($P = 0.004$, 0.0005, and 0.00008, respectively) [6,7]. Eight weeks after gene transfer, such aminergic deficits were markedly ameliorated ($P = 0.022$, 0.0007, and 0.0004 vs. untreated PKU, respectively; Fig. 2b). Accordingly, the levels of some catecholamine metabolites increased in the AAV-treated mice. In PKU mice, 3-4-dihydroxyphenylacetic acid decreased significantly compared with the heterozygous controls, and it recovered partly after gene transfer. 3-methoxytyramine (3-MT) content in PKU mice was not significantly lower than that in the heterozygous controls, but it may have actually been lower compared with WT homozygotes [6]. Otherwise, a compensatory dopamine release to the synapse may take place in PKU mice, resulting in a relatively small 3-MT decrease. As shown in Table 1, we found a significant increase in 3-MT after gene therapy, presumably due to an improved dopamine synthesis. In contrast, homovanillic acid did not increase after gene transfer ($P = 0.749$ vs. PKU; $P = 0.023$ vs. heterozygous). Overall, we assumed that catecholamine synthesis in the AAV-treated mice was restored to approximately 80–90% of the level in heterozygous mice. Similarly, the levels of serotonin and its metabolite 5-hydroxyindoleacetic acid recovered to 60–70% of those in heterozygous mice ($P = 0.039$ for 5-HT and $P = 0.092$ for 5-hydroxyindoleacetic acid).

Fig. 2

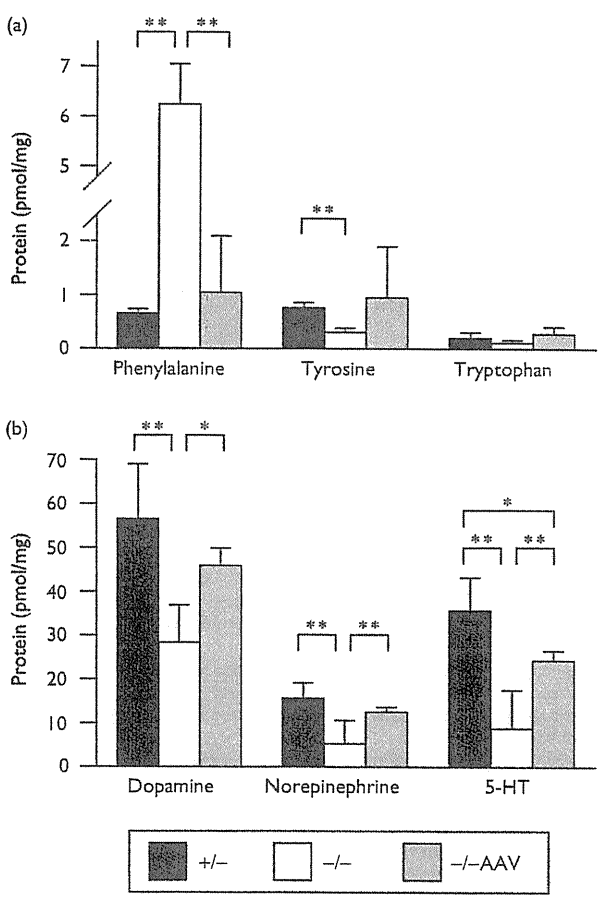

Aromatic amino acids and neurogenic amines in the phenylketonuria (PKU) mouse brain. (a) Phenylalanine, tyrosine, and tryptophan levels in the brain of heterozygous control (+/–), untreated PKU (–/–), and adeno-associated virus (AAV)-treated PKU (–/–AAV) mice. (b) Dopamine, norepinephrine, and serotonin (5-HT) levels in the brain of heterozygous control (+/–), untreated PKU (–/–), and AAV-treated PKU (–/–AAV) mice. Data are shown as the mean ± SD. *$P<0.05$, **$P<0.01$.

Discussion

The present study showed an overt reversal of the aminergic deficit in PKU mouse brain after liver-targeted gene therapy. In untreated PKU mice, HPA may disturb monoamine synthesis through at least two mechanisms. One is that excess phenylalanine may hamper the neuronal uptake of tyrosine (dopamine and norepinephrine precursor) and tryptophan (5-HT precursor) through competition for transport across the blood–brain barrier by the L-type amino acid carrier [14,15]. The other is that a high concentration of phenylalanine interferes with tyrosine hydroxylase and tryptophan hydroxylase [16,17]. For the catecholamine pathway, we observed a significant decrease in the amount of tyrosine in PKU mice, which may play some role in the dopamine and norepinephrine deficit. However, Joseph and Dyer [18] reported an increase in dopamine despite low tyrosine levels in PKU mice on a low-phenylalanine diet, which may suggest that HPA causes a lack of catecholamine primarily by inhibiting the hydroxylation of tyrosine. As for the serotonin pathway, we found a limited decrease in tryptophan in the PKU mouse brain. Pascucci *et al.* [7] found a similar decrease in tryptophan and observed a significant decrease in 5-hydroxytryptophan in the brain of PKU mice. Therefore, they speculated that HPA impedes 5-HT synthesis mainly by inhibiting tryptophan hydroxylation, which is the rate-limiting step in this pathway. We previously showed that phenylalanine acted as an inhibitor more strongly against tryptophan hydroxylase than against tyrosine hydroxylase [17], further

Table 1 Dopamine, norepinephrine, 5-hydroxytryptamine, and metabolites (pmol/mg protein) in adeno-associated virus-treated *Pah*$^{enu2/enu2}$ and control mouse brain

	Pah$^{enu2/+}$ ($n=6$)	*Pah*$^{enu2/enu2}$ ($n=4$)	*Pah*$^{enu2/enu2}$ + adeno-associated virus ($n=3$)
Dopamine	56.6±12.4[a]	28.4±8.5	45.9 ±4.0[a]
3-Methoxytyramine	11.9±4.6	9.9±2.1	13.7±1.2[b]
3-4-Dihydroxyphenylacetic acid	10.4±2.2[a]	4.7±1.2	7.9±1.6[b]
Homovanillic acid	41.9±12.1[b]	25.1±5.1	26.2±2.7[c]
Norepinephrine	15.7±3.5[a]	5.3±1.4	12.5±1.1[a]
5-Hydroxytryptamine	35.8±7.5[a]	8.8±2.5	24.3±2.3[a,c]
5-Hydroxyindoleacetic acid	24.3±7.9[a]	5.3±1.5	15.0±2.0[a]

Values are represented as mean±SD.
[a]$P<0.01$ vs. *Pah*$^{enu2/enu2}$.
[b]$P<0.05$ vs. *Pah*$^{enu2/enu2}$.
[c]$P<0.05$ vs. *Pah*$^{enu2/+}$.

supporting their speculation. By either mechanism, correction of HPA would reset amine metabolism and thereby improve the relevant brain function, as we demonstrated here and previously [8].

Untreated PKU patients have smaller brains, and the primary pathologic finding is hypomyelination and gliosis of central nervous system white matter. A similar pathologic change is observed in *Pah*^{enu2} mice, which may result from aberrant glial cell differentiation induced by HPA [19]. It has also been documented that cerebral protein synthesis is decreased in PKU mice, which presumably contributes to the underdevelopment and degeneration of the PKU brain [13]. We observed a marked recovery in brain weight in the PKU mice only 8 weeks after gene transfer. Correction of HPA may facilitate protein synthesis and reset glial cell plasticity to reconstitute myelin. In addition, it may reduce oxidative stress and induce neuronal regeneration as shown by Embury *et al.* [20].

The results demonstrate that liver-targeted gene therapy for PKU would restore the structural and biochemical fitness of the brain. Current gene transfer technology has achieved a partial reconstitution of coagulation factor IX in the human liver to ameliorate hemophilia B [21]. Further development should lead to broader applications of this modality including PKU. Preventing HPA without a restrictive diet would make it easier to meet nutritional requirements for the physical and neuronal development of patients as well as to maintain sociopsychological well-being.

Conclusion

Liver-targeted gene therapy for PKU reverses the aminergic deficit in the brain and improves the neuropsychological function.

Acknowledgements

The authors thank Mr. Sho Shimaguchi (Tokyo Institute of Technology) for assisting with brain amine analysis and Prof. Kazunao Kondo (Fujita Health University) for assisting with amino acid analysis. They also thank Prof. Hiroyuki Yoshikawa and Dr. Hiromi Hamada (University of Tsukuba) for enthusiastic support and thoughtful discussion. This work was supported in part by Grants-in-Aid for Scientific Research from the Ministry of Education, Culture, Sports, Science and Technology, Japan (20591230).

Conflicts of interest

There are no conflicts of interest.

References

1 Scriver CR, Kaufman S. Hyperphenylalaninemia: phenylalanine hydroxylase deficiency. In: Scriver CR, Beaudet AL, Sly WS, Valle D, editors. *The metabolic and molecular bases of inherited disease.* 8th ed New York: McGraw-Hill. 2001; pp. 1667–1724.
2 McKean CM. The effects of high phenylalanine concentrations on serotonin and catecholamine metabolism in the human brain. *Brain Res* 1972; **47**:469–476.
3 Güttler F, Lou H. Dietary problems of phenylketonuria: effect on CNS transmitters and their possible role in behavior and neuropsychological function. *J Inherit Metab Dis* 1986; **9 (Suppl 2)**:169–177.
4 Shedlovsky A, McDonald JD, Symula D, Dove WF. Mouse models of human phenylketonuria. *Genetics* 1993; **134**:1205–1210.
5 McDonald JD, Charlton CK. Characterization of mutations at the mouse phenylalanine hydroxylase locus. *Genomics* 1997; **39**:402–405.
6 Puglisi-Allegra S, Cabib S, Pascucci T, Ventura R, Cali F, Romano V. Dramatic brain aminergic deficit in a genetic mouse model of phenylketonuria. *NeuroReport* 2000; **11**:1361–1364.
7 Pascucci T, Ventura R, Puglisi-Allegra S, Cabib S. Deficits in brain serotonin synthesis in a genetic mouse model of phenylketonuria. *NeuroReport* 2002; **13**:2561–2564.
8 Mochizuki S, Mizukami H, Ogura T, Kure S, Ichinohe A, Kojima K, *et al.* Long-term correction of hyperphenylalaninemia by AAV-mediated gene transfer leads to behavioral recovery in phenylketonuria mice. *Gene Ther* 2004; **11**:1081–1086.
9 Yagi H, Ogura T, Mizukami H, Urabe M, Hamada H, Yoshikawa H, *et al.* Complete restoration of phenylalanine oxidation in phenylketonuria mouse by a self-complementary adeno-associated virus vector. *J Gene Med* 2011; **13**:114–122.
10 Thöny B. Long-term correction of murine phenylketonuria by viral gene transfer: liver versus muscle. *J Inherit Metab Dis* 2010; **33**:677–680.
11 Kure S, Sato K, Fujii K, Aoki Y, Suzuki Y, Kato S, *et al.* Wild-type phenylalanine hydroxylase activity is enhanced by tetrahydrobiopterin supplementation in vivo: an implication for therapeutic basis of tetrahydrobiopterin-responsive phenylalanine hydroxylase deficiency. *Mol Genet Metab* 2004; **83**:150–156.
12 Sumi-Ichinose C, Urano F, Kuroda R, Ohye T, Kojima M, Tazawa M, *et al.* Catecholamines and serotonin are differently regulated by tetrahydrobiopterin: a study from 6-pyruvoyltetrahydropterin synthase knockout mice. *J Biol Chem* 2001; **276**:41150–41160.
13 Smith CB, Kang J. Cerebral protein synthesis in a genetic mouse model of phenylketonuria. *Proc Natl Acad Sci USA* 2000; **97**: 11014–11019.
14 Shulkin BL, Betz AL, Koeppe RA, Agranoff BW. Inhibition of neutral amino acid transport across the human blood-brain barrier by phenylalanine. *J Neurochem* 1995; **64**:1252–1257.

15 Pietz J, Kreis R, Rupp A, Mayatepek E, Rating D, Boesch C, *et al.* Large neutral amino acids block phenylalanine transport into brain tissue in patients with phenylketonuria. *J Clin Invest* 1999; **103**:1169–1178.
16 Curtius HC, Niederwiesser A, Viscontini M, Leimbacher W, Wagmann H, Blehova B, *et al.* Serotonin and dopamine synthesis in phenylketonuria. *Adv Exp Med Biol* 1981; **133**:277–291.
17 Ogawa S, Ichinose H. Effect of metals and phenylalanine on the activity of human tryptophan hydroxylase-2: comparison with that on tyrosine hydroxylase activity. *Neurosci Lett* 2006; **401**:261–265.
18 Joseph B, Dyer CA. Relationship between myelin production and dopamine synthesis in the PKU mouse brain. *J Neurochem* 2003; **86**:615–626.
19 Dyer CA, Kendler A, Philibotte T, Gardiner P, Cruz J, Levy HL. Evidence for central nervous system glial cell plasticity in phenylketonuria. *J Neuropath Exp Neur* 1996; **55**:795–814.
20 Embury JE, Charron CE, Martynyuk A, Zori AG, Liu B, Ali SF, *et al.* PKU is a reversible neurodegenerative process within the nigrostriatum that begins as early as 4 weeks of age in *Pah*^{enu2} mice. *Brain Res* 2007; **1127**:136–150.
21 Nathwani AC, Rosales C, McIntosh J, Riddel A, Rustagi P, Galder B, *et al.* Early clinical trial results following administration of a low dose of a novel self complementary adeno-associated viral vector encoding human factor ix in two subjects with severe haemophilia B. *Hum Gene Ther* 2010; **21**:1362.

THE JOURNAL OF GENE MEDICINE
J Gene Med 2011;**13**: 114–122.
Published online in Wiley Online Library (wileyonlinelibrary.com) **DOI:** 10.1002/jgm.1543

RESEARCH ARTICLE

Complete restoration of phenylalanine oxidation in phenylketonuria mouse by a self-complementary adeno-associated virus vector

Hiroya Yagi[1,2]
Tsuyoshi Ogura[2]
Hiroaki Mizukami[1]
Masashi Urabe[1]
Hiromi Hamada[2]
Hiroyuki Yoshikawa[2]
Keiya Ozawa[1]
Akihiro Kume[1]*

[1]*Division of Genetic Therapeutics, Center for Molecular Medicine, Jichi Medical University, Shimotsuke, Japan*

[2]*Department of Obstetrics and Gynecology, Institute of Clinical Medicine, University of Tsukuba, Tsukuba, Japan*

*Correspondence to: Akihiro Kume, Division of Genetic Therapeutics, Center for Molecular Medicine, Jichi Medical University, 3311-1 Yakushiji, Shimotsuke 329-0498, Japan
E-mail: kume@jichi.ac.jp

Received: 5 October 2010
Revised: 15 December 2010
Accepted: 24 January 2011

Abstract

Background Classical phenylketonuria (PKU) arises from a deficiency of phenylalanine hydroxylase (PAH) that catalyses phenylalanine oxidation in the liver. Lack of PAH activity causes massive hyperphenylalaninemia and consequently severe brain damage. Preclinical studies showed that conventional adeno-associated virus (AAV) vectors could correct hyperphenylalaninemia in a mouse model of PKU, although limitations such as very large dose requirement and relative inefficiency in female animals were recognized.

Method An AAV8-pseudotyped vector was constructed with a self-complementary AAV (scAAV) genome for efficient liver transduction and expression. Following vector injection to PKU mice, blood Phe was periodically measured by an enzymatic fluorometric assay. *In vivo* Phe oxidation was evaluated by a non-invasive breath test using [1-^{13}C]Phe. Vector copy number in the host tissues was determined by quantitative polymerase chain reaction.

Results A single injection of 1×10^{11}–1×10^{12} particles of the scAAV8 vector resulted in a reduction of blood Phe to normal or near-normal levels for more than 1 year in both genders. The treated animals showed normal level of *in vivo* Phe oxidation. The presence of >1 copy of vector DNA per diploid genome in the liver was associated with normal blood Phe in the AAV-treated PKU mice.

Conclusions Complete phenotypic correction of PKU mice was achieved by the scAAV8 vector for the longest duration reported to date. The vector overcame the female-specific disadvantage in AAV-mediated liver transduction; thus, it offers a promising platform of long-lasting gene therapy for PKU. Copyright © 2011 John Wiley & Sons, Ltd.

Keywords adeno-associated virus; gene therapy; phenylketonuria; phenylalanine oxidation

Introduction

Phenylketonuria (PKU; OMIM 261 600) is an autosomal recessive disorder caused by a deficiency of phenylalanine hydroxylase (PAH; EC 1.14.16.1) in the liver [1]. The enzyme is responsible for the major part of phenylalanine (Phe) clearance by converting Phe to tyrosine (Tyr) with the aid of tetrahydrobiopterin (BH_4) and molecular oxygen. Consequently, PAH deficiency leads to a massive accumulation of Phe under a normal

diet, which is toxic to the developing brain. Untreated patients are afflicted with severe mental retardation, seizure and growth failure, as well as hypopigmentation of the hair and skin. The current management for PKU mandates an early diagnosis by newborn screening followed by a Phe-restricted diet to prevent irreversible brain damage in infancy and childhood. Such a diet is also recommended for adult PKU patients to avoid problems associated with hyperphenylalaninemia, such as psychomotor dysfunction and teratogenic effects on fetuses carried by the female patients (so-called 'maternal PKU syndrome'). However, the unpalatable and expensive diet loads heavy burdens on the patients and their families. Therefore, an alternative approach to PKU, preferably achieving a life-long cure, is desired.

We and other investigators have explored the development of somatic gene therapy for PKU, which offers a novel therapeutic paradigm [2,3]. The most straightforward approach is to deliver the functional PAH gene to the liver, where the enzyme is normally expressed. In most preclinical studies, a mouse model of PKU (*Pah*^{enu2} strain developed in BTBR background) has been used because it shows a similar phenotype to human PKU [4,5]. Thus far, recombinant adeno-associated virus (AAV) vectors have shown the most promising results in correcting hyperphenylalaninemia in *Pah*^{enu2} mice [6–10]. Through these studies, however, two major problems were recognized. One was the relatively large dose requirement of AAV vectors to correct murine PKU phenotype compared to other disease models such as haemophilia B. The other problem was gender-dependent effectiveness of AAV vectors, particularly when they were targeted to the liver. That is, female *Pah*^{enu2} animals required greater AAV doses to reduce blood Phe, and the therapeutic effect was not long-lasting. This phenomenon was investigated in some detail with another animal model [11]. To enhance gene delivery and overcome these problems, attention has turned to alternative AAV serotypes with distinct tissue tropism (e.g. AAV8 for liver transduction) [12–14]. Pseudotyping with AAV8 capsid showed higher efficiency in treating *Pah*^{enu2} mice, together with *cis*-acting elements to enhance liver-specific transcription and mRNA transport [9,10].

In the quest for a further improvement in liver transduction, we realized that another drawback in AAV transduction should be circumvented. Because the single-stranded (ss) DNA genomes of conventional AAV vectors are transcriptionally inactive, they must become double-stranded (ds) to be expressed. The ss- to dsDNA conversion requires host cell-mediated DNA synthesis or annealing of complementary genomes from separate virions, which appears to be the rate-limiting step in AAV transduction [15,16]. This process can be bypassed with a self-complementary (sc) AAV vector because its genome DNA spontaneously self-anneals to form stable dsDNA in the host cell [17–19]. Therefore, we investigated the efficacy of a self-complementary AAV (scAAV) vector for the treatment of *Pah*^{enu2} mice.

Materials and methods

Vector construction

A serotype 8-pseudotyped ssAAV vector for PKU (ssAAV8/CAG-mPAH) was constructed with ssAAV/CAG-mPAH plasmid (Figure 1, top) used in our previous study [7,20]. A scAAV8 vector was constructed with scAAV/LP1-hFIX plasmid carrying the human factor IX (hFIX) gene (kindly provided by Dr John T. Gray, St Jude Research Hospital, Memphis, TN, USA) [21]. For vector-derived PAH expression, the hFIX sequence (*Eco*R I-*Xho* I) in scAAV/LP1-hFIX was replaced with the murine PAH (mPAH) cDNA (*Eco*R I-*Sal* I) from ssAAV/CAG-mPAH (Figure 1, bottom). AAV8-pseudotyoed vector stocks were propagated by an adenovirus-free, three-plasmid transfection method [22]. Briefly, a 10-tray Cell Factory container (CF10; Nalge Nunc International, Rochester, NY, USA) of semiconfluent 293 cells were cotransfected with 650 μg of AAV/CAG-mPAH or scAAV/LP1-mPAH plasmid, 650 μg of AAV2 rep-AAV8 cap helper plasmid (pRep-Cap8 from Dr J. M. Wilson [12]) and 650 μg of adenoviral helper plasmid (pAdeno [23]) by standard calcium phosphate method. Cells were incubated with active gassing for 3 days and harvested [24]. AAV vectors were purified from the crude cell extract by serial ultracentrifugation with CsCl. Vector genome (vg) titers were determined by dot blot hybridization with the mPAH cDNA probe [7]. For scAAV8/LP1-mPAH, titration was also carried out by quantitative polymerase chain reaction (qPCR), where scAAV8/LP1-mPAH and the vector plasmid standard were amplified with a primer set (5′-ACAGTGAATCCGGACTCTAAGG-3′ and 5′-CTGCTCAGGACTCCGTTCTC-3′) using a real-time PCR instrument (7900HT; Applied Biosystems, Foster City, CA, USA). A 136-bp region between LP1 promoter and the mPAH cDNA was amplified and confirmed by agarose gel electrophoresis. The qPCR-based titer was calibrated with the result of other titration methods described previously [25,26].

Animals and gene delivery

Colonies of a PKU model mouse, BTBR-*Pah*^{enu2} and its wild-type (WT) strain BTBR (obtained from Jackson Laboratories, Bar Harbor, ME, USA) were maintained in the animal facility of Jichi Medical University. All animals were fed standard mouse chow (CE-2 from Clea Japan, Tokyo, Japan) *ad libitum* providing approximately 25% of energy as protein. Genotyping for the presence of the *Pah*^{enu2} mutation was performed by PCR analysis of tail biopsy DNA. In brief, exon 7 (136 bp) of the mPAH gene was amplified with a primer set (5′-CTTGTACTGGTTTCCGCCTC-3′ and 5′-GG TTCAGGTGTGTACATGGG-3′). The amplified DNA from WT allele is cleaved by *Mbo*II into 70-bp and 66-bp fragments, whereas the counterpart from *Pah*^{enu2} allele is uncleavable as a result of the c.835T → C (F263S) mutation [5]. The scAAV vector (1×10^{11} to 3×10^{12}

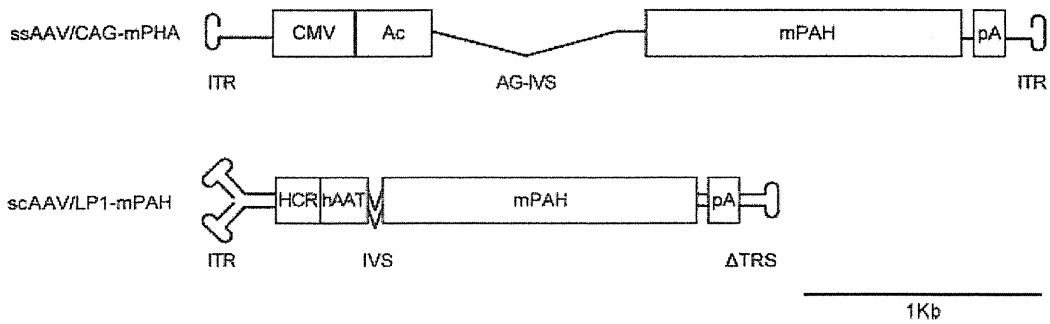

Figure 1. Structure of AAV vectors for PKU gene therapy. Top: ssAAV/CAG-mPAH vector. CAG promoter consists of the human cytomegalovirus immediate-early enhancer (CMV), the chicken β-actin promoter (Ac) and a chicken β-actin/rabbit β-globin composite intron (AG-IVS). CAG promoter, the murine phenylalanine hydroxylase cDNA (mPAH) and the SV40 late polyadenylation signal (pA) are flanked by the AAV inverted terminal repeats (ITR). Bottom: scAAV/LP1-mPAH vector. LP1 promoter consists of the human apolipoprotein E/C-I hepatic control region (HCR) and the human α1-antitrypsin promoter (hAAT). In addition, the vector contains a modified SV40 small t-antigen intron (IVS), mPAH and pA. The entire expression cassette is flanked by the intact AAV ITR and the terminal resolution site-deleted ITR (ΔTRS)

particles) was dissolved in 0.5 ml of saline and injected into the peritoneal cavity of *Pah*^{enu2} mice. All animal experiments were carried out in accordance with the institutional guidelines under protocols approved by the Institutional Animal Care and Use Committee at Jichi Medical University.

Blood Phe assay

Blood Phe was measured by an enzymatic fluorometric assay using an Enzaplate PKU-R kit (GE Healthcare, Tokyo, Japan) [7]. Mice were tail phlebotomized and 30–40 μl of blood was spotted onto a paper filter (No. 545 for newborn mass screening; Advantec Toyo, Tokyo, Japan). A disc (3 mm in diameter) was punched out from the dried blood spot and placed in a round-bottom, 96-well microtiter plate. Phe was eluted from the disc and incubated with resazurin and Phe dehydrogenase, an NAD-dependent enzyme. The enzyme reaction produces NADH, which in turn converts resazurin to resorufin with the aid of diaphorase. The resultant resorufin was measured on a Fluoroskan Ascent plate reader (Labsystems, Helsinki, Finland) with a 544 nm/590 nm filter set.

Evaluation of *in vivo* Phe oxidation

In vivo Phe oxidation activity was evaluated by a method of Kure *et al.* [27] with slight modification. [1-^{13}C]L-Phe (^{13}C-Phe; from Cambridge Isotope Laboratories, Andover, MA, USA) and L-Phe (from Wako Pure Chemicals, Osaka, Japan) were dissolved in saline at 200 mg/ml and 20 mg/ml, respectively, and sterilized through 0.22-μm syringe filters (Millex-GV, Millipore, Yonezawa, Japan) immediately before intraperitoneal (i.p.) injection. Mice were preloaded with 20 mg/kg of L-Phe 30 min prior to ^{13}C-Phe challenge (2 mg/kg). Each mouse was kept in a lid-sealable plastic box for 15 min before and 45 min after ^{13}C-Phe challenge, and a total volume of 120 ml of air was transferred to a sampling bag for [^{13}C]urea breath test (Otsuka Pharmaceuticals, Tokyo, Japan) with a glass syringe. The ratio of $^{13}CO_2$ and $^{12}CO_2$ was measured by gas chromatography-mass spectrometry (GC-MS; by SRL, Tokyo, Japan), and the difference was designated as $\Delta^{13}CO_2$.

Determination of vector biodistribution

Tissue genomic DNA was extracted by a standard method using proteinase K (Boehringer Manheim, Manheim, Germany) and phenol:chloroform (Nippon Gene, Toyama, Japan). To quantify genomic DNA copy number, a unique region of the murine β-actin gene was amplified by qPCR with a primer set (5′-GGTCCTGG ATCACTCAGAACGGACACCA-3′ and 5′-AGCCTCAATAC GCACGCGCAGCTAAC-3′) along with a plasmid control. Vector copy number in tissue DNA was estimated by qPCR in the same manner as in vector titration.

Statistical analysis

Statistical analysis was performed using StatView, version 5.0, for Macintosh (SAS Institute, Cary, NC, USA). A paired *t*-test and unpaired *t*-test (Student's *t*-test or Welch's *t*-test) were used for comparison between the two groups. $p < 0.05$ was considered statistically significant for all analyses.

Results

Construction of AAV8 vectors for PKU

For comparison with scAAV8, a reference ssAAV8 vector was constructed with ssAAV/CAG-mPAH plasmid (Figure 1, top) [7]. Although the CAG promoter allowed very high hepatic expression in our previous studies

with ssAAV2 and ssAAV5 [7,28], the size of CAG-mPAH expression cassette (3.5 kb) exceeded the limit of packaging capacity of a scAAV vector (up to 2.2 kb). To meet the packaging requirements of scAAV, Nathwani *et al.* [21] developed a compact hFIX expression cassette (LP1-hFIX; 2.1 kb) and assembled it in the modified AAV2 backbone with an intact 5′ terminal resolution site (*trs*) and a deleted 3′ *trs* (scAAV/LP1-hFIX). The LP1 hybrid enhancer/promoter consists of the core liver-specific elements from the human apolipoprotein E/C-I gene hepatic control region (HCR) and the human α1-antitrypsin promoter (hAAT). The expression cassette also contains a modified SV40 small t-antigen intron and the SV40 late polyadenylation signal. Because the coding sequences of mPAH (1362 bp) and hFIX (1386 bp) have almost identical lengths, we constructed scAAV/LP1-mPAH vector by replacing the hFIX cDNA in scAAV/LP1-hFIX with the mPAH cDNA from ssAAV/CAG-mPAH (Figure 1, bottom). PAH expression from the resultant plasmid (scAAV/LP1-mPAH) was confirmed by transfection of Huh7 cells and immunoblotting (data not shown). The ssAAV/CAG-mPAH and scAAV/LP1-mPAH genomes were packaged into AAV serotype 8 capsid and titrated by dot blot hybridization. The determined titers of viral stocks were approximately 1×10^{13} vg/ml for ssAAV8/CAG-mPAH and 6×10^{13} vg/ml for scAAV8/LP1-mPAH, respectively. scAAV8/LP1-mPAH was also titrated by qPCR along with a plasmid control and calibrated with the result obtained from dot blot hybridization [25].

Efficacy of ssAAV8 in PKU mice

We previously reported that 1×10^{13} vg of ssAAV5/CAG-mPAH partially corrected hyperphenylalaninemia in male *Pah*^{enu2} mice when administered through the portal vein (PV) [7]. Meanwhile, ssAAV8 vectors delivered reporter genes to adult mouse liver with comparable efficiency following either i.p. or intravenous injection, with an apparent gender-specific barrier [29,30]. Therefore, we administered a log-smaller dose (1×10^{12} vg) of ssAAV8/CAG-mPAH vector to the peritoneal cavity of male PKU mice. This procedure resulted in an almost complete correction of hyperphenylalaninemia for 24 weeks (Figure 2a), confirming a very efficient liver transduction by AAV8. This observation prompted us to carry out a similar comparative study with female *Pah*^{enu2}. When female PKU mice were given 1×10^{13} vg of ssAAV8/CAG-mPAH through PV, blood Phe was rapidly decreased to normal levels (<2 mg/dl), and the initial impact on blood Phe was identical to that of PV-injected 1×10^{14} vg of ssAAV5/CAG-mPAH (Figure 2b). The therapeutic effect was transient, however, and hyperphenylalaninemia gradually resumed to the pretreatment level by 24 weeks post-injection. The same dose (1×10^{13} vg) of i.p.-injected ssAAV8/CAG-mPAH exhibited minimal effect on blood Phe during the observation period (Figure 2b). Taken together, the liver transduction efficiency of the ssAAV8 vector was

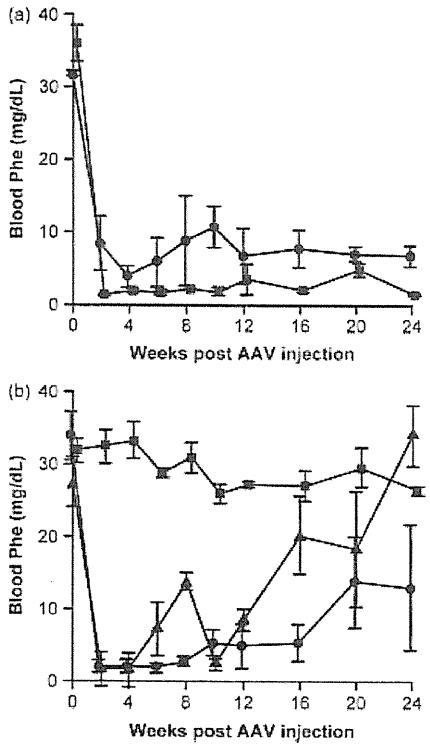

Figure 2. Efficacy of ssAAV5 and ssAAV8 vectors in *Pah*^{enu2} mice. (a) Male *Pah*^{enu2} mice were given either 1×10^{13} vg of ssAAV5/CAG-mPAH through the portal vein (PV) (circles, $n = 4$; data adopted from Mochizuki *et al.* [7]), or 1×10^{12} vg of ssAAV8/CAG-mPAH by i.p. (squares, $n = 3$). Blood Phe (mg/dl) levels are shown as the mean ± SD. (b) Female *Pah*^{enu2} mice were given either 1×10^{14} vg of ssAAV5/CAG-mPAH via the PV (circles, $n = 5$; data adopted from Mochizuki *et al.* [7]), 1×10^{13} vg of ssAAV8/CAG-mPAH via the PV (triangles, $n = 4$), or 1×10^{13} vg of ssAAV8/CAG-mPAH by i.p. injection (squares, $n = 3$). Blood Phe (mg/dl) levels are shown as the mean ± SD

greater than that of ssAAV5 by tenfold, although the gender-specific barrier was not overcome. Regarding the administration route of AAV8, PV injection was superior to i.p. injection, although the latter procedure was useful in male mice.

Short-term efficacy of scAAV8 in Phe metabolism of female PKU mice

Based on the above result with the ssAAV8 vector, we realized that further improvement was required to cure female *Pah*^{enu2} mice. Therefore, we addressed whether the self-complementary AAV genome would boost liver transduction. We gave 1×10^{11} or 1×10^{12} vg of scAAV8/LP1-mPAH to the peritoneal cavity of adult female *Pah*^{enu2} (8 weeks of age). These doses were two to three logs smaller than those of ssAAV5 and ssAAV8 vectors showing a transient therapeutic effect on female *Pah*^{enu2} (Figure 2b). When fed standard chow, the blood Phe concentration in WT BTBR mice was below 1.7 mg/dl (100 μM), whereas that in untreated *Pah*^{enu2} mice was above 20 mg/dl (1200 μM) (Table 1).